AN ABSTRACT OF THE THESIS OF

NENG-CHUN YAO (Name) for the M. S. (Degree)

in Oceanography (Major) presented on May 9, 1967 (Date)

Title: ANALYSIS OF HYDROGRAPHIC TECHNIQUES -- A STUDY OF DIFFERENT EFFECTS ON GEOSTROPHIC CURRENT COMPUTATIONS BY USING VARIOUS HYDROGRAPHIC DATA PROCESSING METHODS

Abstract approved: Redacted for privacy
Stephen J. Neshyba

The effects of five data processing methods on the accuracy of geostrophic computations are analyzed using hydrographic data collected from a set of 24 hour triangular stations off the Oregon coast. Sources of error are assessed by comparison with an available in situ Salinity/Temperature/Depth record (STD) trace at a control station.

The results of this study show that the accuracy of the dynamic depth anomaly depends on the choice of vertical integration intervals based on sea water density distribution instead of on an arbitrary set of standard depths for all the cases, and that the effect of interpolation of hydro-data is not significant if the data is properly sampled and adequately interpolated.

Some sources of error in computations of geostrophic currents

from hydrographic data can be alleviated by proper sampling and processing procedures. They are (1) the sampling errors caused by improper sampling schemes which miss the sharp features and periodic variations (i. e. internal waves) in the ocean, and (2) processing errors caused by improper interpolations of data and determinations of mean density.

Analysis of Hydrographic Techniques -- A Study of Different Effects on Geostrophic Current Computations by Using Various Hydrographic Data Processing Methods

by

Neng-chun Yao

A THESIS

submitted to

Oregon State University

in partial fulfillment of
the requirements for the
degree of

Master of Science

June 1967

APPROVED:

Redacted for privacy

Professor of Oceanography
In Charge of Major

Redacted for privacy

Chairman of Department of Oceanography

Redacted for privacy

Dean of Graduate School

Date thesis is presented May 9, 1967

Typed by Marcia Ten Eyck for Neng-chun Yao

ACKNOWLEDGEMENT

I would like to express my deep appreciation to Dr. Wayne V. Burt, Chairman of the Department of Oceanography, for providing me the valuable opportunity of studying oceanography in the United States. Special acknowledgement is due to Dr. Stephen J. Neshyba, my major professor. Without his encouragement and assistance, my study in oceanography would never have been successful.

I wish to extend my gratitude to Mr. William Quinn who devoted much of his time to provide valuable suggestions on researching and English writing, and to Mr. Walt Pawley for his assistance in computer programming.

Also, I am greatly indebted to the Office of Naval Research and the National Science Foundation, through whose support the data used in this study were collected, and to the members of the Department of Oceanography who participated in the data collection operation.

I owe special thanks to my wife, Shiu-chin, for her never failing understanding and encouragement during her lonely years in Taiwan while I was absent from home studying in the United States.

TABLE OF CONTENTS

LIST OF FIGURES

LIST OF TABLES

LIST OF SYMBOLS

α	= specific volume of sea water, in cm^3/gm
$\alpha_{s, t, p}$	= specific volume of sea water <u>in situ</u>, in cm^3/gm
$\alpha_{s, t, o}$	= specific volume of sea water at salinity in ‰, temperature in ^oC and atmosphere pressure cm^3/gm
$\alpha_{35, 0, p}$	= specific volume of sea water at salinity 35 ‰, temperature 0^oC and pressure p in decibars, in cm^3/gm
$\alpha_{35, 0, 0}$	= specific volume of sea water at salinity 35 ‰, temperature 0^oC and atmosphere pressure, equal to 0.972643 cm^3/gm
cl	= the quantity of chlorine in parts per mille (‰) of weight
δ	= specific volume anomaly, in cm^3/gm
$\bar{\delta}$	= mean specific volume anomaly, in cm^3/gm
δ_s	= salinity term
δ_t	= temperature term
δ_{st}	= temperature and salinity term
δ_{sp}	= salinity and pressure term
δ_{tp}	= temperature and pressure term
Δ_{st}	= thermosteric anomaly, in centiliter/ton or cm^3/gm
$\bar{\Delta}_{st}$	= mean thermosteric anomaly, in centiliter/ton or cm^3/gm
Δ	= finite difference
ΔD	= dynamic depth (or height) anomaly, in dynamic meters or centimeters
dyn. cm	= dynamic centimeter
db	= decibars

f = coriolis parameter, in per second

$\hat{k}$ = unit vector perpendicular to horizontal plane

L = distance between stations, in meters or centimeters

p = pressure in decibars

$\nabla_H P$ = horizontal pressure gradient, in dynes/cm^3

$\rho_{s, t, p}$ = sea water density in situ, in gm/cm^3

$\rho_{s, t, o}$ = sea water density at salinity in ‰, temperature in ^oC, and atmosphere pressure, in gm/cm^3

$\rho_{35, 0, 0}$ = sea water density at salinity 35‰, temperature 0^oC, and atmosphere pressure, in gm/cm^3

σ_t = sigma-t = $(\rho_{s. t. o}-1)\ 1000$

σ_0 = value of sigma-t when t is zero

$\sigma_{35. 0. 0}$ = sigma-zero = $(\rho_{35. 0. 0}-1)\ 1000 = 28.126$

R = scale factor accounting for vertical exaggeration on vertical section

τ = acceleration potential, in cm^2/sec^2

ϕ = geopotential anomaly, in cm^2/sec^2

S = salinity in parts per mille (‰) of weight

t = temperature in ^oC

A_t, B_t, Σ_t = temperature parameters used in the basic formulae for calculating the in situ specific volume anomaly

V_H = magnitude of the relative horizontal current normal to a line joining the two stations, in meter/sec or cm/sec

ω = angular velocity of the earth, in radian/sec

θ = mean latitude between stations, in degrees

$\tan \beta$ = slope of isanosteric contour

Z = depth in meters

Σ = summation

ANALYSIS OF HYDROGRAPHIC TECHNIQUES -- A STUDY OF DIFFERENT EFFECTS ON GEOSTROPHIC CURRENT COMPUTATIONS BY USING VARIOUS HYDROGRAPHIC DATA PROCESSING METHODS

I. INTRODUCTION

This paper is a study of the effects on accuracy of computed geostrophic currents due to the use of different practical methods of processing hydrographic data. A large amount of hydro-data has been processed by various organizations using different methods. Although these methods now in use each has special virtues, a study of their errors and applicability in certain circumstances will provide a basis for judging the validity of their results and for choosing a suitable method in performing certain oceanic observations.

The possible associated sources of error in dynamic computation of geostrophic current are (1) accelerations in the current system being studied, (2) deviations of the selected reference from a level surface, (3) frictional influences, (4) instrument effects (temperature, salinity and pressure), (5) improper correcting of instrument reading, (6) improper plotting, interpolating of data and selecting of mean densities, (7) inadequate sampling, (8) internal waves, (9) deviations in ion ratios, and (10) drawing of topography contours (Leipper, 1959). The different hydro-data processing methods incorporate to various extents these possible sources of error, except those inherent systematic errors such as accelerations

in the current system, reference level, frictional influence, and instrument and measurement errors. Therefore, in this study, these exceptions will be excluded. The magnitudes of these systematic errors have been studied by several oceanographers, and their findings are assumed to be correct and are used as references in this study.

A brief review of methods of dynamic computation of geostrophic current is included to show the important role of the processing procedure involved. The discussion of theorems and problems concerned in hydro-data processing is followed by comparisons of the calculated magnitudes of the sea water density, geopotential anomaly, dynamic depth anomaly, and the current by those methods studied.

II. REVIEW OF METHODS OF DYNAMIC COMPUTATION

Dynamic computation of geostrophic current is based on the following assumptions: (1) the horizontal pressure gradient is balanced by the Coriolis force, (2) the horizontal velocity and the horizontal pressure gradient vanish at a moderate depth below the sea surface and (3) the field accelerations and frictional forces can be neglected (Sverdrup, 1947). These assumptions simplify the equation of motion into the so-called geostrophic equation

$$(1) \quad -f \hat{k} \times \hat{V}_H - \alpha \nabla_H P = 0$$

where f = Coriolis parameter, in $1/sec$

V_H = Horizontal current velocity, in cm/sec

α = Specific volume of sea water, in cm^3/gm

$\nabla_H P$ = Horizontal pressure gradient, $dynes/cm^3$

$$= \frac{\partial P}{\partial x} + \frac{\partial P}{\partial y}$$

$\hat{k}$ = Unit vector perpendicular to horizontal plane

Since no method is known by which the slope of the pressure surface can be measured, several methods have been developed to compute the horizontal pressure gradient in terms of different obtainable parameters. Those methods often used by oceanographers are the geopotential scheme, acceleration potential scheme and isanosteric contour slope scheme.

Geopotential Scheme

On the basis of Bjerknes' circulation theorem (1900), Sandström and Helland-Hansen (1903), (as cited by Fomin, 1964), obtained a formula for computing current velocities at particular horizons from the distribution of sea water density.

(2) $$\frac{10\,(\Delta D_A - \Delta D_B)}{L} = V_H 2\omega \sin\theta$$

where $\Delta D_A - \Delta D_B$ = difference in the anomalies of dynamic height at stations A and B, in dynamic meters

(3) $\Delta D = \int_{p_2}^{p_1} \delta\, dp$ is used to obtain dynamic height. For practical calculation, ΔD is obtained from the numerical expression

(4) $\Delta D = \sum_i \bar{\delta}_i \Delta p_i$, where Δp is pressure in decibars and $\bar{\delta}_i$ is mean specific volume anomaly in the i th pressure interval, in 10^{-5} cm^3/gm.

L = distance between stations in meters

V_H = magnitude of the relative current normal to a line joining the two

stations in m/sec.

ω = angular velocity of the earth, equal to 0.729×10^{-4} radians per second.

θ = mean latitude between stations.

Acceleration Potential Scheme

Montgomery and Stroup (1962) developed a scheme using the quantity "acceleration potential" which is $(\phi + \delta p)$ and represented by T. The expression for obtaining relative current is given as

$$(5) \qquad V_H = \frac{\Delta T}{f\,L}$$

where $f = 2\omega \sin \theta$, the coriolis parameter, in 1/sec.

L = distance between stations, in cms.

V_H = magnitude of the relative current normal to a line joining the two stations, in cm/sec.

(6) ΔT = acceleration potential anomaly in cm^2/sec^2, given by $(\phi + \delta_1 p_1)_A - (\phi + \delta_1 p_1)_B$, where ϕ is geopotential anomaly in cm^2/sec^2, and $\delta_1 p_1$ is taken at the reference level, also in cm^2/sec^2.

or $\Delta T = \left(\int_{\delta_1}^{\delta_2} p\,d\delta + \delta_1 p_1\right)_A - \left(\int_{\delta_1}^{\delta_2} p\,d\delta + \delta_1 p_1\right)_B$ in cm^2/sec^2,

δ is specific volume anomaly in cm^3/gm and

p is pressure in decibars.

For practical calculation, numerical integration is used and the expression for obtaining relative current then has the form:

$$(7) \qquad V_H = \frac{(\sum_i \bar{p}\,\Delta\delta + p_1\delta_1)_A - (\sum_i \bar{p}\,\Delta\delta + p_1\delta_1)_B}{fL}$$

where pressure p in decibars is generally replaced by depth in meters.

Isanosteric Contour Slope Scheme

Werenskjöld (1935, 1937), (as cited by Neshyba and Amstutz, 1965), introduced a method to compute the relative current velocity field by summing the slopes of isanosteric contours. According to Montgomery and Wooster's investigation (1954), in constructing the isanosteric contours of vertical sections, the thermosteric anomaly Δ_{st} may be used instead of specific volume anomaly in the upper 500 db or 1000 db level. The resultant sum is then in the common geostrophic equation

$$(8) \quad f(V_2 - V_1) = \int_{\delta_1}^{\delta_2} \left(\frac{dp}{dx}\right)_\delta d\delta$$

where $\left(\frac{dp}{dx}\right)_\delta$ is the slope of isanosteric contour.

A convenient method and instrument for computing the relative current velocity with this scheme has been developed by Neshyba et al. (1965). If the isanosters are contoured with uniform small

increments (for instance $\Delta(\Delta_{st}) = 10$ centiliter/ton), the geostrophic current can be readily obtained by

$$(9) \quad V_1 - V_2 = \frac{R\ \Delta(\Delta_{st})}{f} \sum_i \tan \beta$$

where R is a scale factor accounting for vertical exaggeration of the section and $\tan \beta$ is the slope of the insanosteres as measured with the special instrument mentioned.

The unique feature of this scheme is that the relative current is obtainable at any particular point on the vertical section. One can choose the point at a station or between stations. Another special feature is that the effects of vertical variation of density caused by internal waves, etc. are often apparent on the isanosteric contours. From the shape of the contours, a ready check of reliability of hydro-data is provided. A bad data point often causes unusual variation in the contours.

III. HYDRO-DATA PROCESSING SCHEMES USED IN DYNAMIC COMPUTATION OF GEOSTROPHIC CURRENT

The Role of Hydro-data Processing in Dynamic Computation

With present Nansen bottle and thermometer sampling schemes, the first step in all dynamic geostrophic computation methods is to obtain the specific volume anomaly δ or thermosteric anomaly Δ_{st} (which can be used in all methods mentioned) from the value of temperature t and salinity S at observed depths. Due to the fact that the actual depths of observations do not usually coincide with the "standard depths" (these are an internationally established set of depth intervals for reporting hydrographic data), a certain interpolation procedure has to be employed to reduce the measured values of t and S to the corresponding values at standard depths. δ or Δ_{st} data are calculated from these reduced t and S data. The various methods for computing geostrophic current are based on numerical or graphical integration to obtain the geopotential or acceleration potential anomaly at the stations.

As assumed in the introduction, the errors in instrument and measurement are considered to be fixed. Wooster and Taft (1958) examined the measurement error in the geopotential anomaly of the upper 1000 meters (0-1000 db) and concluded that the error in dynamic depth anomaly difference between two stations is $\pm$ 1.1 dyn

cm. But, Reed and Laird (1966) found that with the modern salinometer, the measurement error would be $\pm$ 0. 3 dyn. cm. Both of these findings are used in this study as references for evaluating the errors caused by the several computational procedures. These procedures play an important role in computation and are the main features of studying different hydro-data processing methods. The same set of data when processed in different ways often yields different results in geostrophic current.

As the geopotential scheme is a well accepted method in oceanic investigation (LaFond, 1951), the study of effects due to different hydro-data processing methods is based on this scheme.

The Basic Formulae Used in Hydro-data Processing

The classical equations of determining sea water density developed by Knudsen (1901, cited by Bjerknes and Sandström, 1910) and Bjerknes and Sandström (1910) are the basic formulae for calculating the in situ specific volume anomaly (LaFond, 1951).

Those basic equations are as follows:

(10) $S = 0.030 + 1.805\ cl$ (Knudsen, 1901)

where S = salinity in parts per mille (‰) of weight.

cl = the quantity of chlorine in parts per mille (‰) of weight.

(11) $\sigma_o = -0.069 + 0.4708\ cl - 0.001570\ cl^2 + 0.0000398\ cl^3$

(12) $\sigma_t = \Sigma_t + (\sigma_o + 0.1324)\ [1 - A_t + B_t\ (\sigma_o - 0.1324)]$

where σ_o is an expression of sea water density in situ, expressed by

$(\rho_{s,t,o} - 1) \times 1000$ (Bjerknes et al., 1910)

where $\rho_{s,t,o}$ is sea water density of in situ salinity and temperature, and atmospheric pressure.

σ_o is the value of σ_t where $t = 0$

$$\Sigma_t = -\frac{(t - 3.98)^2}{503.570} \times \frac{t + 283}{t + 67.26}$$

$$A_t = t\ (4.7867 - 0.09815t + 0.0010843\ t^2)10^{-3}$$

$$B_t = (18.030 - 0.8164\,t + 0.01667\ t^2)10^{-6}$$

t = temperature in ^oC

(13) $$\alpha_{s,t,p} = \alpha_{s,t,o} - P\alpha_{s.t.o}10^{-9}\left\{\frac{4886}{1+0.0000183p} - [227 + 28.33t - 0.551t^2 + 0.004t^3] + P\,10^{-4}\,[105.5 + 9.50t - 0.158t^2] - 1.5P^2t\,10^{-8} - \frac{\sigma_o - 28}{10}\,[147.3 - 2.72t + 0.04t^2 - P10^{-4}\,(32.4 - 0.87t + 0.002t^2)] + \left(\frac{\sigma_o - 28}{10}\right)^2 [4.5 + 0.1t - P10^{-4}(1.8 - 0.6t)]\right\}$$

where $\alpha_{s,t,p}$ = specific volume of sea water in situ, in cm^3/gm

$\alpha_{s, t, o}$ = specific volume of sea water of salinity in parts per mille (‰), temperature in ^{o}C and atmospheric pressure in cm^3/gm

p = pressure in decibars

(14) $\delta = \alpha_{s, t, p} - \alpha_{35, p, o}$

where δ = specific volume anomaly, cm^3/gm

$\alpha_{35, o, p}$ = specific volume of sea water of salinity 35‰, temperature $0^{o}C$, and at a pressure of p decibars, in cm^3/gm.

(15) $$\alpha_{35, o, p} = \alpha_{35, o, o} - P\,\alpha_{35, o, o}\left[\frac{4886}{1+0.0000183P} - 22\right] + 0.01055P-(\sigma_{35. o. o}-28)(14.73-0.000324P)]10^{-9}$$

where $\alpha_{35, o, o}$ = specific volume of sea water at salinity 35‰, temperature $0^{o}C$ and atmospheric pressure equal to 0.972643 cm^3/gm.

$\sigma_{35, o, o}$ = sigma-zero, equal to 28.126.

(16) $\delta = \Delta_{st} + \delta_{sp} + \delta_{tp}$ (Sverdrup, 1933, cited by LaFond, 1951)

where Δ_{st} = thermosteric anomaly

$$= 0.0273596 - \frac{10^{-3}\sigma_t}{1-10^{-3}\sigma_t}, \text{ in } cm^3/gm.$$

δ_s = salinity term

δ_t = temperature term

δ_{st} = temperature and salinity term

δ_{sp} = salinity and pressure term

δ_{tp} = temperature and pressure term.

All the pressures in decibars in the above equations can be replaced by corresponding values of depth in meters (LaFond, 1951).

Practical Schemes for Hydrographic Data Processing

Hydro-Tables H. O. Pub. No. 614

Based on the above mentioned formulae, LaFond (1951) compiled a set of tables, called H. O. tables, and procedures for simplifying the reduction of hydro-data. A few sets of tables provide means to obtain Δ_{st}, δ_{sp}, δ_{tp}, and σ_t values from entries of t, S, and p. The specific volume anomaly is obtained by formula (16).

A numerical vertical integration of formula (4) yields the dynamic depth (or height) anomaly of one horizon relative to another. There are also other tables for correcting thermometers, etc.

These tables are adopted for standard procedures of hydrographic data reduction by the U. S. Navy and are also widely used by oceanographic institutions.

Computer Programs

The use of a digital computer greatly simplifies the processing of hydrographic data. With suitable programs, it can perform the processing of huge amounts of hydro-data with very high accuracy. It is widely used wherever a computer is available. However, different programs do yield certain differences in the end result.

Hans Klein Chart

Klein (1955) invented a graphic technique for processing and presenting oceanographic data. The graphic tool, called the Hans Klein Chart, provides

1. A clear graphic picture of uniformly analyzed data with minimum expenditure of time.
2. A speedy mechanical rather than computational procedure to produce both sigma-t and Δ_{st} as functions of depth.

This scheme is also widely adopted as a tool for processing data at sea.

There are some other schemes such as the use of Knudsen tables and graphic methods by Sund and Calloway (LaFond, 1951). Due to the fact that they are not in general use, they are not included in this study.

IV. PRACTICAL PROBLEMS IN HYDRO-DATA PROCESSING PROCEDURE

The Nansen bottle method of hydrographic sampling is still in general use. The inherent nature of this type of sampling poses certain difficulties in the processing of hydro-data. The difficulties are mainly due to the fact that this sampling method is unable to detect the detail in actual variations of temperature and salinity caused by the somewhat periodic changes of oceanic factors by tides and internal waves. Therefore, it cannot provide a continuous distribution of temperature, salinity and density of sea water with respect to depth. Hence, the use of interpolation in the data reduction is necessary.

Effect of Discrete Vertical Sampling of Temperature and Salinity

Defant (1950) pointed out that the often neglected aspect in hydrographic sampling of the nearly periodic variations of temperature and salinity (as well as other oceanographic factors) may actually result in worthless observations and erroneous conclusions. In fact, he observed that the disturbance caused by tides can reach a maximum of 8.0 dyn-cm which is much higher than the overall measurement error of 1.1 cyn-cm (Wooster and Taft, 1958). He further stated that the variations might be due to internal waves with a tidal

period, or, in the case of larger horizontal temperature and salinity gradients, they might be caused by the horizontal advection of different water bodies.

Recent observations with Bathythermographs (BT traces) by Konaga (1965) show that internal waves excited by the tidal-generating force, oceanic currents, wind or atmospheric pressure distribution cause a depth fluctuation of the isotherms which in turn produces a depth fluctuation in the isopycnal surfaces. According to his study, the variation of dynamic depth anomaly occurs mainly in the upper 500 meter layer where the oceanic sharp thermocline usually exists. Also, the study shows a case where the difference in dynamic depth anomalies due to internal waves is about ten dyn. cm, and the corresponding change of computed surface geostrophic current is about 1.3 knot. From actual current measurements using a Geomagnetic Electrokinetograph (GEK), he found a variation in surface current of about 0.8 knot which was in fair agreement with that from the calculated current. Although his study was unable to analyze the actual characteristics of periodic variation, it confirms that the BT trace could detect the variation of ispycnal surfaces in the upper layer.

It seems feasible that BT information can supplement bottle sampling data. A BT trace taken during the time when a hydro-cast is made is used to get the actual profile of temperature in the upper 250 meters by transferring the BT trace onto the vertical profile

obtained from the observed bottle data. This is done by hand plotting. The temperature readings picked from the translated BT trace at the place where changes of curvature appear are used to smooth the bottle data and to achieve better definition of the temperature structure in the upper layer. Corresponding salinity data is not obtained, and one is forced to rely on bottle salinity data. The values so obtained can be used in all hydro-data processing methods, but the effect in end result is yet to be checked.

Defant (1950) proposed a program of survey to eliminate the semi-diurnal internal wave completely. However, due to usual oceanographic cruise conditions, it is not practical to space the stations so rigidly that all of them are occupied at the same phase time of the internal wave. Also, it is not necessarily desirable to overlook these variations as in some cases the variation itself is an interesting subject for study. According to Reed and Laird (1966), in order to achieve the best results station spacing should vary in different water masses. Thus Defant's proposed method is not practical in the general case. Therefore, the variations caused by internal wave effects are usually inherent in sampled data. It seems that they may cause some doubt about the reliability of the results computed from these data. This study is an effort to find the practical effect on accuracy due to missing such details.

The Error Associated with the Interpolation of Hydro-Data

As pointed out, a certain interpolation procedure is used to reduce the measured values of temperature and salinity (or specific volume anomaly) at observed depths to standard depths. Oceanographers have used graphic interpolation for this purpose (Lafond, 1951; Leipper, 1957). However, since computer processing has become general practice, the use of quadratic interpolation is necessary. The Lagrange and Log methods are used by United States (U. S. Navy Hydrographic Office, 1960) and Canadian (Fraese, 1960) oceanic institutions, respectively. Linear interpolation is also used by some oceanographers.

Bulgakov and Moroz (1965) found that the actual values of temperature and salinity might be greater or less than the corresponding values of the quantities reduced to standard depths. Thus, the difference between current speeds calculated on the basis of in situ specific volume at standard and observed depths may reach three to four cm per second, and the relative magnitude may differ as much as 50 percent. In some cases a current calculated from temperature and salinity adjusted to standard depths may be opposite to a current calculated by direct adjustment of the in situ specific volume to standard depth. They suggest that these errors might be avoided by interpolating the values of in situ specific volume instead of

temperature and salinity.

However, an earlier study by the U. S. Naval Hydrographic Office (1960) found no significant difference between the interpolated values by computer using Lagrange or Log scheme and those by graphical scheme. A comparison was also made between interpolated sigma-t values and those computed from interpolated temperature and salinity. The differences are extremely small. This finding shows clearly that if a suitable interpolation scheme is used, the problem presented by Bulgakov et al., (1965) might not be serious. This aspect is also a part of this study.

An improvement of the Lagrange interpolation scheme has been made by using the average of the values obtained from two Lagrange interpolation polynomials: one polynomial uses two points above and one below the depth of interpolation, and the other uses one point above and two points below this depth. This improved scheme gives a better interpolated value over a wider range of conditions than the others that have been proposed. It also allows an error of interpolation to be determined (Rattray, 1961). Hence, this scheme has been widely accepted by various institutions including the Department of Oceanography at Oregon State University, and is used in the computer programs of this study.

The Error Associated with Numerical Integration

The geopotential dynamic computation method uses a numerical integration to obtain dynamic heights (or depths) (Lafond, 1951), given by formula (4). The error caused by substituting depth in meters for pressure in decibars is considered insignificant as it amounts to only one percent or less (LaFond, 1951). However, the choice of the interval ΔZ does affect the mean specific volume anomaly, $\bar{\delta}$. The average of the boundary values may not represent the real mean value of δ in the interval, as the variation of δ between two depths is not linear. A rapid change of specific volume anomaly often exists in the region of the thermocline. Only the use of small intervals can make the boundary averaged value approach to the real mean value. Based on known continuous profiles of temperature and salinity, a quantitative comparison of the difference in interval choice is included in this paper.

V. COMPARISONS OF THE EFFECTS IN ERROR OF DIFFERENT HYDRO-DATA PROCESSING METHODS

Quantitative comparisons are made to analyze the applicability of the different hydro-data processing methods in dealing with practical problems discussed in preceding sections. Sea water density and dynamic depth anomaly, calculated from several sets of data using five different methods arranged from the three practical hydro-data processing schemes, are analyzed. The effects, on accuracy of computed geostrophic current due to the practical problems in data processing, are analyzed in Chapter VI.

Description of the Processing Methods

First Method

This method uses the FORTRAN, L, X, computer program of oceanographic data processing (sequence 447) which is used by the Department of Oceanography, Oregon State University, for routine data processing (Appendix I). This program includes two parts: in the first part, the measured values of temperature and salinity at observed depths are reduced to the interpolated values at standard depths by Rattray's improved Lagrange interpolation method, i. e., using average value of two Lagrange interpolation polynomials (see Chapter IV). The second part computes sigma-t and converts

it into specific volume $\alpha_{s,t,p}$ at standard depth from the interpolated temperature and salinity values, using the classical equations (Bjerknes and Sandström, 1910). It then obtains the specific volume anomaly, δ, by subtracting sea water specific volume $\alpha_{35,o,p}$ at standard depth from that calculated in situ, $\alpha_{s,t,p}$. The dynamic depth is then found by formula (4).

Second Method

This method is used to analyze the difference between the current calculated from temperature and salinity interpolated to standard depths and current calculated from direct interpolation of observed in situ specific volume anomaly to standard depths.

This method employs a new FORTRAN, L, X, computer program (sequence 852) which is specially arranged for this study (Appendix II). This program first computes sigma-t and specific volume from the observed temperature and salinity values. Specific volume anomaly δ is obtained as in the first method, and the same interpolation method is used to reduce the values of specific volume anomaly δ at observed depths to those at standard depths; also, the same numerical method is used to compute the dynamic depth anomaly.

In this method, only one interpolation procedure is used up to the step of obtaining dynamic depth. The temperature and salinity values at standard depth are also interpolated to standard depths,

but for reference purposes only. The interpolation program is arranged slightly differently from the one in the first method to reduce computer time, but it is the same improved scheme of Lagrange interpolation.

Third Method

This method uses the same FORTRAN L, X, program as the second method. But its input not only contains values of thermometer temperature and salinity but also temperature data obtained from bathythermographs. These additional data are the temperature values picked from BT temperature profiles and the salinity values picked from smoothly curved salinity profiles at corresponding depths. In this way, greater detail of the actual temperature structure is taken into account and more values are provided for interpolation. The sigma-t and dynamic depth anomaly values so obtained are compared with those obtained from the other methods to analyze the effect of missing temperature detail in the upper layer.

Fourth Method

The Hans Klein chart (Appendix III) is used in this method. It provides a quick way to obtain sigma-t and thermosteric anomaly by plotting temperature and salinity value at each observed depth (Klein, 1955). This method follows these steps:

1. Plot the temperature vs. depth curve, with the aid of a BT trace to get the best available vertical temperature structure in the upper layer where the sharp thermocline usually appears.
2. Plot salinity vs. depth curve.
3. Plot the T-S (temperature vs. salinity) curves using values at observed depths and those values picked from vertical salinity and temperature profiles at the depths where detail in temperature variation is desired, especially at the depth of a sharp thermocline.
4. A smooth vertical profile of Δ_{st} and σ_t based on observed depths is obtained by means of graphic interpolation.
5. From the continuous vertical Δ_{st} profile, a simple, small interval numerical integration for dynamic depth can be used, since the values of depth interval ΔZ and mean thermosteric anomaly $\overline{\Delta_{st}}$ are easily obtained from the vertical profiles (Figure 1).

The choice of the ΔZ is arbitrary. It can be made between standard depths or any pair of depths. In the area of sharp curvature, a small interval of five meters is used to enhance the accuracy of finding the mean value of the thermosteric anomaly. Then, dynamic depth anomaly is obtained by formula (4). The dynamic depth anomaly so obtained does not include the part contributed by

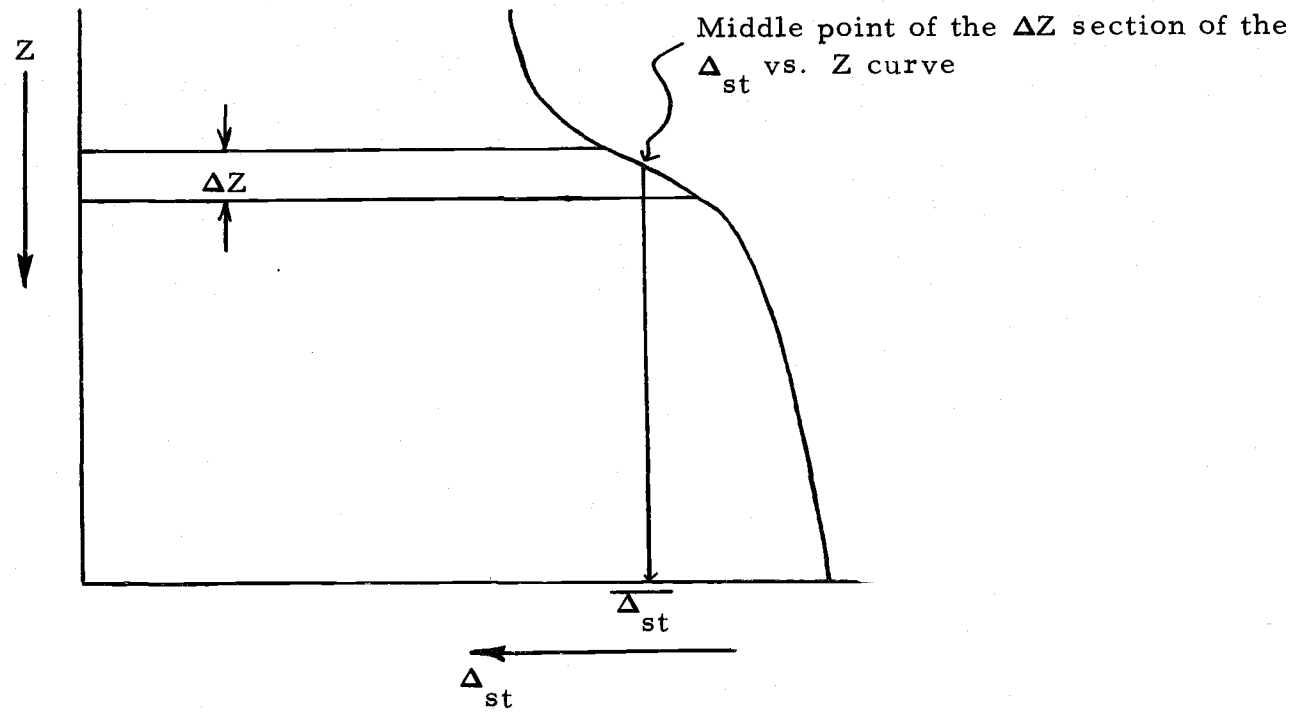

Figure 1. Graphic Method of Finding ΔZ and $\overline{\Delta_{st}}$ From Hans Klein Chart.

the pressure terms which is considered negligible in up to 1000 meter depths (Montgomery and Wooster, 1954).

Fifth Method

Hydro-tables (H. O. 614) are used in this method to calculate the value of specific volume anomaly δ from temperature and salinity at observed depth. From Table V-A, V-B, V-C thermosteric anomaly Δ_{st} is obtained. Then, the pressure terms δ_{tp} and δ_{sp} are obtained from Tables VI and VII, respectively. The sum of Δ_{st}, δ_{tp} and δ_{sp} yields specific volume anomaly at observed depth.

The δ vertical profile is plotted on the Hans Klein Chart using the same scale as for Δ_{st}. Then, the vertical profile is shaped into a smooth curve using the plotted Δ_{st} profile obtained from the same set of data on the same chart as a reference curve. Since the value of δ in the upper 200 meter layer is almost equal to that of Δ_{st}, the δ profile in that region almost coincides with the Δ_{st} profile which includes the detailed upper-layer temperature structure; thus, the δ profile so obtained also includes this detail indirectly.

The geopotential depth anomaly ΔD is obtained by the same means as in the fourth method. This method takes care of almost all the problems discussed in Chapter IV provided that the small linear interpolations used in entering temperature and salinity values from the tables do not cause substantial errors. This will be checked out

by comparing the value of δ obtained from tables and that directly calculated from the equations by computer. The difference between the end result of this method and that of the Hans Klein chart is due to the contribution of pressure terms.

Sources of Data Used

24-Hour Triangular Station Data from R/V YAQUINA Cruise 6611 31 October - 6 November 1966

In this cruise, triangular sets of 24-hour stations were occupied as shown in Figure 2. A total of 18 separate casts were made at these stations. From these, four sets were obtained such that the times of casts within each set were about the same time of day as shown in Table 1.

The four sets of data are processed using each of the five methods outlined in the preceding subsection. An analysis of the different effects on dynamic current computation by using the various hydro-data processing techniques is made in Chapter VI.

Station 11, Boreas Expedition (University of California, 1966)

The STD ("in situ Salinity/Temperature/Depth Recorder") temperature and salinity traces at this station are similar to the temperature and salinity profiles obtained at the 24-hour triangle stations (Figure 3). With the assumption that these traces are the real

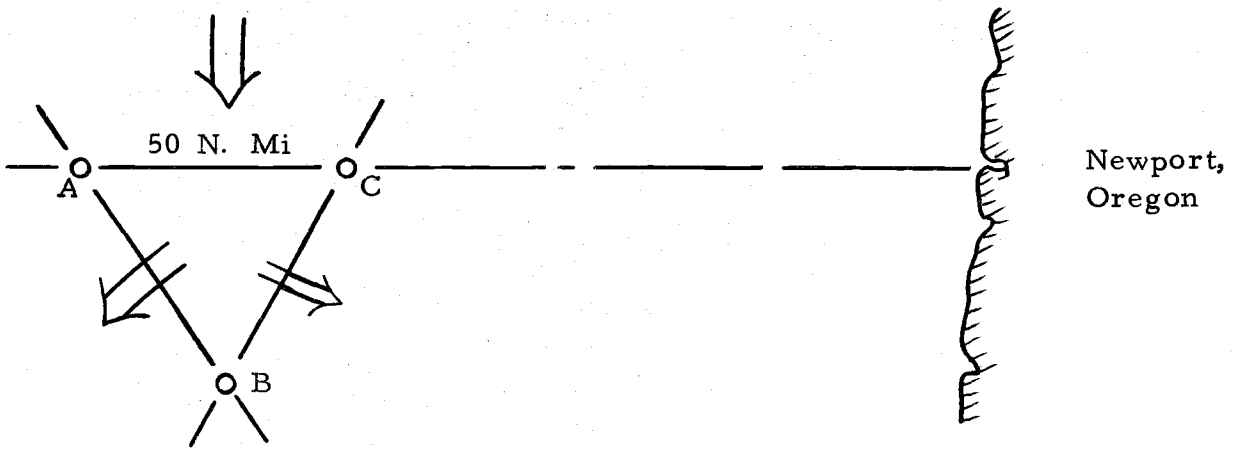

Figure 2. Location of Three 24 Hour Hydrographic Stations, Spaced 50 N. Mi off Newport, Oregon Coast, November 2-6, 1966.

Table 1. Time Distribution of Four Data Sets From Three 24-Hour Hydrographic Stations.

Set	Station	Cast No.	Date	Time
1	HA	1	2 Nov.	1945
	HB	3	4 Nov.	1939
	HC	1	5 Nov.	2205
2	HA	2	2 Nov.	2155
	HB	4	4 Nov.	2228
	HC	2	6 Nov.	0000
3	HA	3	2 Nov.	2346
	HB	5	5 Nov.	0150
	HC	3	6 Nov.	0155
4	HA	4	3 Nov.	0400
	HB	6	5 Nov.	0547
	HC	4	6 Nov.	0430

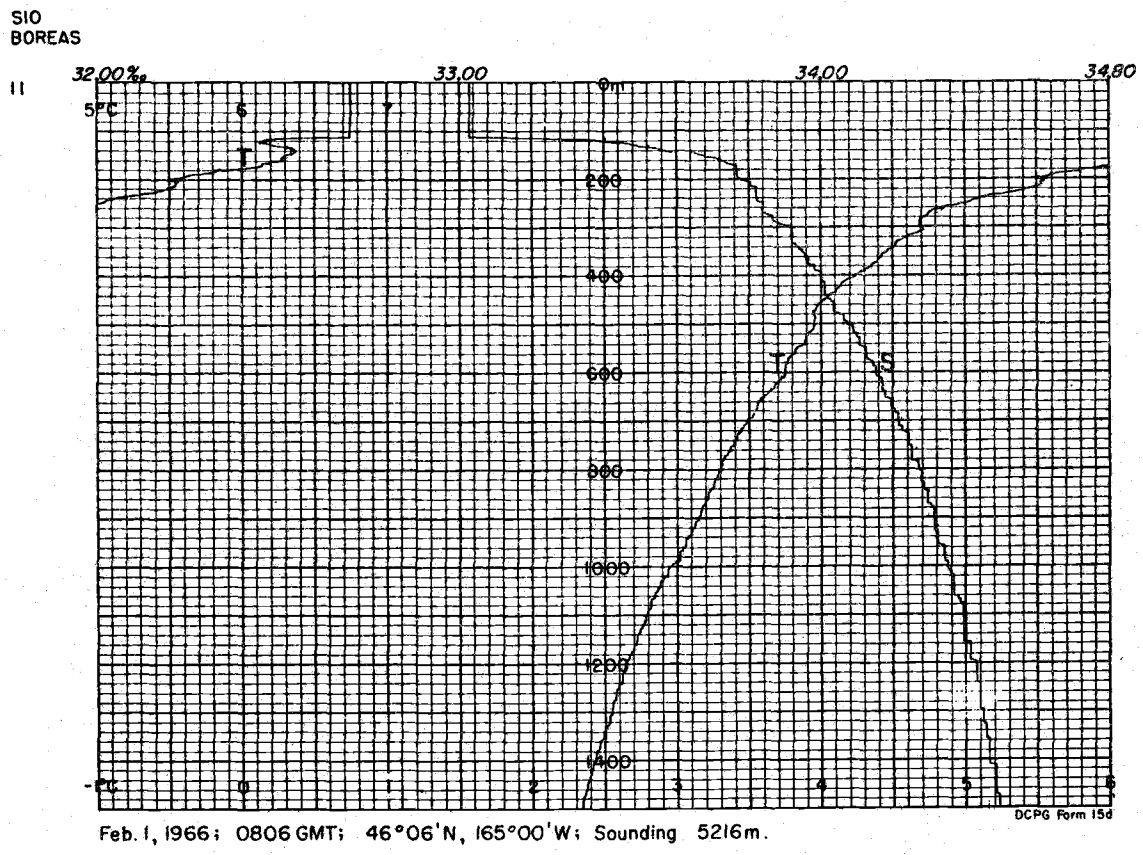

Figure 3. STD Temperature and Salinity Traces at Station 11 of the Boreas Expedition.

oceanic structure of sea water, they are used to provide a basis for judging the applicability of the hydro-data processing methods to be studied. The Boreas data, then, is a "control" station for this analysis.

Station 44, 45, in the Study of Bulgakov et al. (1965)

The available data of stations 44 and 45 used in the study of Bulgakov et al. are also processed with the first and second methods in this study to assess the difference between linear interpolation and the improved Lagrange interpolation in hydro-data processing.

Comparisons

Obtaining Accurate Sea Water Density Values

The digital computer process in methods one, two, and three directly applies the basic formulae to calculate the sigma-t and specific volume anomalies from sea water temperature, salinity, and pressure. The several sets of tables in H. O. 614 require certain linear interpolations of these quantities to fit their tabulated entries and the results are not obtained directly from the formulae. The graphic scheme of the Hans Klein Chart needs visual interpolation to plot the data points on its spaced scales; also, it only provides sigma-t and the thermosteric anomaly instead of the specific volume anomaly.

For the purpose of checking relative errors, an assumption is

made that the results obtained by the computer are correct, and they are used as the standards for comparison purposes. Table 2 shows the values of sigma-t, specific volume anomaly, thermosteric anomaly and dynamic depth anomaly obtained by the three different processing schemes from a set of 45 small interval data points taken off the STD traces at station 11 of the Boreas Expedition. From column 2, there are 15 differences between the sigma-t values obtained by computer and by H. O. tables. They appear at depths ranging from the sharp thermocline at 122 meters to more than 1000 meters. The maximum deviation value is 0.04, at 140 meters depth. But, at this same depth, the difference between the σ_t values obtained by computer and by the Hans Klein chart is only 0.01; further, the deviation of the Hans Klein set never exceeds 0.01. It appears that the Hans Klein graphic scheme yields more accurate results than does the more time consuming H. O. tables scheme.

However, the Hans Klein chart yields only thermosteric anomaly, and the dynamic depth anomaly, ΔD, obtained from this value does not include the pressure effect. At this station a difference of 0.1 dyn cm appears at 140 meters depth, reaches 1.0 dyn cm at 400 meters, and 5.4 dyn cm at 1200 meters depth. The percentages of the deviations from computer calculated values are 0.04%, 1.61%, and 4.12%, respectively. These are well within the limits of the estimated five percent error in dynamic depth due to omitting the

Table 2. Values of Sigma-t, Specific Volume Anomaly, Thermosteric Anomaly and Dynamic Depth Anomaly Obtained by Three Different Data Processing Schemes From a Set of 45 Small Interval Data Points Taken Off the STD Trace at Station 11 of the Boreas Expedition.

1			2			3			4		
Z Meters	t °C	S ‰	σ_{t1}	σ_{t2}	σ_{t3}	δ_1	δ_2 10^{-5} cm^3/gm	Δ_{st}	ΔD_1 dyn. cm.	ΔD_2 dyn. cm.	ΔD_3 dyn. cm.
0	6.70	33.04	25.94	25.94	25.94	207.4	207.4	207.4	0	0	0
10	6.70	33.04	25.94	25.94	25.94	207.6	207.6	207.4	2.1	2.1	2.1
20	6.70	33.04	25.94	25.94	25.94	207.7	207.6*	207.4	4.2	4.2	4.2
30	6.70	33.04	25.94	25.94	25.94	207.8	207.7*	207.4	6.2	6.2	6.2
50	6.70	33.04	25.94	25.94	25.94	208.1	208.1	207.4	10.4	10.4	10.4
75	6.70	33.04	25.94	25.94	25.94	208.4	208.4	207.4	15.6	15.6	15.6
100	6.70	33.04	25.94	25.94	25.94	208.8	208.6*	207.4	20.8	20.8	20.7*
112	6.70	33.04	25.94	25.94	25.94	208.9	208.8*	207.4	23.3	23.3	23.2*
122	6.15	33.40	26.33	26.32*	26.33	172.3	171.3*	170.7	25.2	25.2	25.1*
140	6.35	33.66	26.47	26.43*	26.46*	158.6	162.7*	158.0	28.2	28.2	28.1*
150	6.33	33.68	26.49	26.49	26.49	157.0	156.8*	154.9	29.8	29.8	29.6*
175	5.75	33.74	26.61	26.61	26.61	145.7	145.5*	143.6	33.6	33.6	33.4*
198	5.52	33.75	26.65	26.65	26.65	142.5	142.4*	140.2	36.9	36.9	36.6*
200	5.50	33.75	26.65	26.65	26.65	142.3	142.2*	140.0	37.2	37.2	36.9*
210	5.55	33.80	26.68	26.67*	26.69*	139.3	139.0*	136.5	38.6	38.6	38.3*
220	5.41	33.82	26.71	26.72*	26.71	136.2	136.3*	133.5	39.9	39.9	39.7*
250	5.00	33.83	26.77	26.77	26.78	131.1	131.2*	128.0	44.0	44.0	43.6*
275	4.70	33.86	26.83	26.83	26.83	125.7	125.7	123.1	47.2	47.2	46.7*
300	4.70	33.92	26.88	26.88	26.88	121.5	121.6*	118.6	50.3	50.3	49.7*
310	4.70	33.92	26.88	26.88	26.89*	121.6	121.6	117.0	51.5	51.5	50.9*
335	4.50	33.92	26.90	26.90	26.91*	119.6	119.5*	115.0	54.5	54.5	53.8*
350	4.46	33.96	26.93	26.93	26.93	116.3	116.3	113.0	56.3	56.3	55.5*
355	4.40	33.97	26.95	26.93*	26.94*	115.0	114.9*	113.0	56.8	56.8	55.6*
375	4.40	33.98	26.96	26.95*	26.96	114.4	114.5*	111.0	59.1	59.1	58.3*
400	4.25	34.00	26.99	27.00*	26.99	111.5	111.1*	106.9	62.0	62.0	61.0*
410	4.14	34.01	27.01	27.02*	27.01	109.6	108.6*	105.1	63.1	63.1	62.1*
425	4.11	34.02	27.02	27.02	27.02	108.7	107.6*	105.0	64.7	64.7	63.7*
450	4.05	34.04	27.04	27.04	27.04	106.8	106.7*	103.0	67.4	67.4	66.3*
475	3.92	34.04	27.05	27.06*	27.05	105.6	105.5*	102.0	70.0	70.0	68.8*
500	3.95	34.08	27.08	27.08	27.08	103.1	103.1	98.9	72.7	72.7	71.4*
550	3.85	34.12	27.12	27.13*	27.12	99.5	98.8*	95.5	77.7	77.7	76.2*
600	3.75	34.15	27.16	27.16	27.16	96.5	96.7*	91.8	82.6	82.6	80.8*
625	3.70	34.15	27.16	27.16	27.16	96.2	96.1	91.8	85.0	85.0	83.2*
650	3.60	34.20	27.21	27.22*	27.21	91.6	91.0*	86.0	87.4	87.3*	85.4*
680	3.59	34.20	27.21	27.21	27.21	91.7	91.7	86.4	90.1	90.1	88.0*
700	3.48	34.22	27.24	27.24	27.24	89.2	89.2	83.9	91.9	91.9	89.7*
750	3.40	34.24	27.26	27.26	27.26	87.2	87.2	81.7	96.3	96.3	93.8*
800	3.30	34.28	27.30	27.30	27.30	83.5	83.5	77.8	100.6	100.6	97.8*
850	3.20	34.31	27.34	27.33*	27.34	80.5	80.5	74.5	104.7	104.7	101.6*
900	3.13	34.31	27.34	27.35*	27.35*	80.1	80.4*	74.4	108.7	108.7	105.4*
950	3.08	34.32	27.36	27.35*	27.36	79.1	79.3*	72.8	112.7	112.7	109.0*
1000	3.00	34.35	27.39	27.39	27.39	76.3	76.5*	69.9	116.6	116.6	112.6*
1065	2.86	34.38	27.43	27.42*	27.43	73.0	73.2*	66.5	121.4	121.4	121.4*
1100	2.78	34.39	27.44	27.44	27.45	71.6	71.1*	64.0	124.0	124.0	119.3*
1200	2.64	34.42	27.48	27.48	27.48	68.4	68.4	61.6	131.0	131.0	125.6*

σ_{t1}, δ_1, ΔD_1 = Calculated by computer

σ_{t2}, δ_2, ΔD_2 = Obtained from H. O. tables

σ_{t3}, δ_3, ΔD_3 = Obtained from Hans Klein chart

* = Values deviating from the one calculated from computer

pressure term specified by Montgomery and Wooster (1954).

Due to the rough interpolation involved in obtaining the pressure terms, δ_{tp} and δ_{sp}, from H. O. tables, the specific volume anomaly values obtained from H. O. tables differ from those obtained by computer (Table 2, column 3). The deviation ranges from a minimum value of 0.1×10^{-5} cm^3/gm to a maximum of 1×10^{-5} cm^3/gm. A total of 31 such differences appears in this computation. But, the dynamic depth anomalies calculated from these two different sets of δ are essentially the same. Only one deviation exists at 650 meters depth. Its value is 0.1 dyn cm which is not significant. Evidently, the dynamic depth anomalies, ΔD, are not sensitive to the variations in specific volume anomaly caused by interpolations in the H. O. table data processing scheme. However, the time saving and error-proof nature of the computer scheme make it preferable to the H. O. tables scheme.

The Effects of Reducing Measured Values at Observed Depths to Values at Standard Depths

The sigma-t, specific volume anomaly, and dynamic depth values obtained by computer and the thermosteric anomaly and dynamic depth anomaly values obtained by the Hans Klein chart from the 45 data points picked off continuous STD traces (Table 2) are considered to be actual *in situ* values in oceanic structure at station 11. Those

values are used as the basis for comparison, and are called "actual in situ" values in this study.

A pseudo-Nansen bottle sampling cast is constructed from the continuous STD traces at this station. The temperature and salinity values are read off the STD traces at the depths where the observed depths usually appear in the ordinary hydro-cast. This set of data is called pseudo-cast hydro-data (Table 3, column A).

The STD temperature trace in the upper 273 meter layer is considered to be the BT trace. From it, four additional temperature readings are picked at various depths. These temperature values as well as the corresponding salinity values picked from the smoothly curved salinity profile with the pseudo salinity data are used to form another set of data (Table 3, column B). This set of data is supposed to supplement the pseudo-cast hydro-data with detailed temperature variation in the upper layer.

The first set of data is processed by the first and second methods and the second set of data is processed by the third and fourth methods. As the fifth method uses the same graphical interpolation as the fourth one, it is not included in this comparison. The values of sigma-t and dynamic depth anomaly at standard depths obtained by these four methods as well as the "actual in situ" values are given in Tables 4A and 4B.

Table 3. Pseudo-cast Hydro-data at Station 11 of the Boreas Expedition.

A			B		
Z	t	S	Z	t	S
0	6.70	33.04	0	6.70	33.04
20	6.70	33.04	20	6.70	33.04
48	6.70	33.04	48	6.70	33.04
72	6.70	33.04	72	6.70	33.04
98	6.70	33.04	98	6.70	33.04
150	6.33	33.68	112*	6.70	33.18
198	5.52	33.75	112*	6.15	33.29
247	5.02	33.83	140*	6.35	33.54
300	4.70	33.92	150	6.33	33.68
398	4.27	34.00	198	5.52	33.75
494	5.02	34.07	220*	5.50	33.78
596	3.76	34.15	247	5.02	33.83
791	3.29	34.27	275	4.71	33.87
990	3.00	34.34	300	4.70	33.92
1189	2.66	34.41	398	4.27	34.00
			494	3.95	34.07
			596	3.76	34.15
			791	3.29	34.27
			990	3.00	34.34
			1189	2.66	34.41

* Additional temperature readings from BT trace.

From Table 4A, it is clear that the first method does not give good results for sigma-t values. Nine values do not agree with the "actual in situ" values, and two such values have a difference of +0.02. The other methods have only four deviations each, with only one +0.02 difference by the second method and only ±0.01 differences in all cases by the third and fourth methods. This comparison shows that, to obtain the most accurate values of sigma-t at standard depths, the interpolation procedure should be applied to the values of density calculated from temperature and salinity values at observed depths instead of to the values of temperature and salinity at observed depths first. The additional data points provided by BT also help to achieve good results as shown in the sigma-t values obtained by the third and fourth methods. There is no significant difference between Lagrangian and graphical interpolation procedures in this aspect.

The Effect of Using Standard Depth Intervals as Integration Intervals

The dynamic depth anomaly values at standard depths obtained by the four methods as well as the corresponding in situ dynamic depth anomaly values are listed in Table 4B. In comparison with the "actual in situ" values one can see that all deviations of dynamic depth anomaly are less than 0.5 dyn cm. The deviations begin at the 150 meter depth where the rapid change of temperature vs. depth occurs,

Table 4A. Comparison of Sigma-t Values at Standard Depths by Various Methods from Pseudo-cast Hydro-data at Station 11 of the Boreas Expeditions.

Z	$\sigma_{t(STD)}$	σ_{t1}	σ_{t2}	σ_{t3}	σ_{t4}
0	25.94	25.95*	25.94	25.94	25.94
10	25.94	25.94	25.94	25.94	25.94
20	25.94	25.95*	25.94	25.94	25.94
30	25.94	25.94	25.94	25.94	25.94
50	25.94	25.94	25.94	25.94	25.94
75	25.94	25.96*	25.94	25.94	25.93*
100	25.94	25.96*	25.96*	25.94	25.95
150	26.49	26.50*	26.49	26.50*	26.49
200	26.65	26.66*	26.65	26.65	26.65
250	26.77	26.78*	26.78*	26.78*	26.78*
300	26.88	26.88	26.88	26.88	26.88
400	26.99	26.99	26.99	26.99	26.99
500	27.08	27.08	27.08	27.08	27.08
600	27.16	27.17*	27.16	27.17*	27.16
700	27.24	27.24	27.24	27.24	27.24
800	27.30	27.31*	27.30	27.30	27.30
1000	27.39	27.39	27.38*	27.38	27.38*
1200	27.48	27.48	27.47*	27.47*	27.47*

$\sigma t(STD)$ = "Actual in situ values" of sigma-t directly from STD traces (Table 2).

σ_{t1}, σ_{t2}, σ_{t3}, σ_{t4} = Sigma-t values at standard depths by first four methods, respectively.

* = Sigma-t values deviating from the "actual in situ σ_t values.

Table 4B. Comparison of Dynamic Depth Anomaly Values in Dyn. Cm at Standard Depths by Various Methods from Pseudo-cast Hydro-data at Station 11 of the Boreas Expedition.

Z	$\Delta D_{(STD)}$	ΔD_1	ΔD_2	ΔD_3	$\Delta D'_{(STD)}$	ΔD_4
0	0	0	0	0	0	0
10	2.1	2.1	2.1	2.1	2.1	2.1
20	4.2	4.2	4.2	4.2	4.2	4.2
30	6.2	6.2	6.2	6.2	6.2	6.2
50	10.4	10.4	10.4	10.4	10.4	10.4
75	15.6	15.6	15.6	15.6	15.6	15.6
100	20.8	20.8	20.8	20.8	20.7	20.8*
150	29.8	29.9*	29.9*	29.9*	29.6	29.8*
200	37.2	37.4*	37.4*	37.4*	36.9	37.2*
250	44.0	44.2*	44.2*	44.2*	43.6	43.9*
300	50.3	50.2*	50.5*	50.5*	49.7	50.0*
400	62.0	62.1*	62.1*	62.2*	61.0	61.3*
500	72.7	72.9*	72.9*	72.9*	71.4	71.6*
600	82.6	82.9*	82.9*	72.9*	80.8	81.1*
700	91.9	92.2*	92.2*	92.2*	89.7	89.9*
800	100.6	100.8*	100.8*	100.9*	97.8	98.0*
1000	116.6	116.8*	116.9*	116.9*	112.6	112.8*
1200	131.0	131.3*	131.4*	131.5*	125.6	125.9*

$\Delta D_{(STD)}$, $\Delta D'_{(STD)}$ = "Actual in situ values" of dynamic depth anomaly from δ, Δ_{st} respectively (Table 2).

ΔD_1, ΔD_2, ΔD_3, ΔD_4 = Dynamic depth anomaly values by first four methods respectively.

* = ΔD values deviating from "actual in situ" ΔD values.

and at this depth an integration interval of 50 meters is used. The larger differences show up in the results obtained by the third method which gives fairly good agreement in sigma-t values.

Using the "actual in situ" specific volume anomaly values from Table 2, a further comparison is made between the dynamic depth anomaly values obtained from small integration intervals and those obtained with standard depth intervals. These two sets of dynamic depth anomaly values are given in Table 5. It shows that most differences in these two ΔD values are accumulated between the depths of 100 and 250 meters where the vertical temperature and salinity structures change rather rapidly. There are only four standard depths in this layer. The mean specific volume anomaly $\bar{\delta}$ obtained between these four depths are less able to fit the density distribution in this layer than the $\bar{\delta}$ obtained between smaller properly chosen depth intervals.

It appears that the choice of standard depth intervals for integration does not represent the real oceanic structure in every case, and that the choice of integration interval can cause more error in data processing than other factors. This seems to be the reason that the effects of deviations in sigma-t do not show up consistently in dynamic depth anomalies.

Table 5. Difference Between Dynamic Depth Anomaly Values in Dyn. Cm by Small Integration Interval and by Standard Depth Interval Using "Actual In Situ" Specific Volume Anomaly Values at Station 11 of the Boreas Expedition.

Z	$\delta 10^{-5}$ cm^3/gm	ΔD_1	ΔD_2	$\Delta D_1 - \Delta D_2$	$\frac{\Delta D_1 - \Delta D_2}{\Delta D_2}$ %
0	207.4	0	0	0	0
10	207.6	2.1	2.1	0	0
20	207.7	4.2	4.2	0	0
30	207.8	6.2	6.2	0	0
50	208.1	10.4	10.4	0	0
75	208.4	15.6	15.6	0	0
100	208.8	20.8	20.8	0	0
150	157.0	30.0	29.8	0.2	0.60
200	142.3	37.4	37.2	0.2	0.54
250	131.1	44.3	44.0	0.3	0.68
300	121.5	50.6	50.3	0.3	0.60
400	111.5	62.2	62.0	0.2	0.32
500	103.1	73.0	72.7	0.3	0.42
600	96.5	82.9	82.6	0.3	0.36
700	89.2	90.0	91.9	0.3	0.33
800	83.5	100.9	100.6	0.3	0.28
1000	76.3	116.9	116.6	0.3	0.26
1200	68.4	131.3	113.0	0.3	0.23

D_1 = Dynamic depth anomaly in dyn. cm by standard depth integration interval.

D_2 = Dynamic depth anomaly in dyn. cm by small integration interval.

The Difference Between Linear Interpolation and Lagrange Interpolation Procedures

Bulgakov et al. (1965) made a study of the currents calculated on the basis of specific volume values obtained from temperature and salinity values interpolated to standard depths and the specific volume values interpolated from values computed at observed depths. They found differences as large as three to four cm/sec (Table 6, column A) and suggested that these errors might be avoided by interpolating the values of specific volume to standard depths instead of the values of temperature and salinity. They used piecewise linear interpolation in their study.

Using the station 44 and 45 data from Bulgakov et al., interpolating of temperature and salinity to standard depths have been made using the improved Lagrange method. In Figures 4A and 4B these data are compared to the Bulgakov et al. study. It appears that the interpolated values by the improved Lagrange method in most cases fit the graphically interpolated smooth profiles better than those by the linear method presented in Bulgakov et al. study (1963). The latter appear to be wrong in certain places either due to systematical or computational errors.

However, in the layer between the 150 and 300 meter depths at station 44 (Figure 4A), both the temperature and salinity values interpolated by the improved Lagrange method show significant deviations

Figure 4A. Comparison of Various Interpolated Temperature and Salinity Values at Standard Depths (Station 44, Bulgakov and Moroz, 1965).

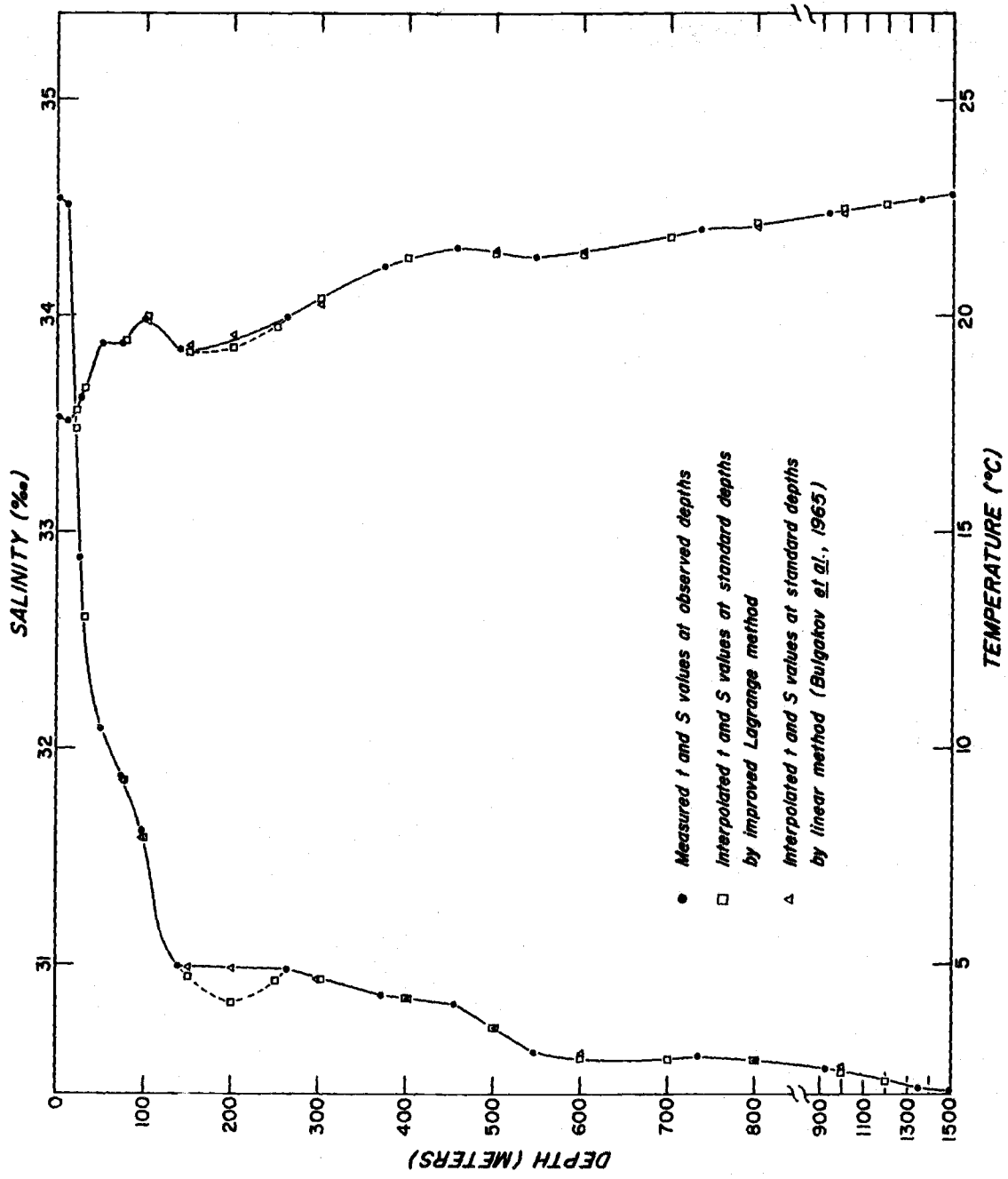
SALINITY (‰)
TEMPERATURE (°C)
DEPTH (METERS)
Measured t and S values at observed depths
Interpolated t and S values at standard depths by improved Lagrange method
Interpolated t and S values at standard depths by linear method (Bulgakov et al., 1965)

Figure 4B. Comparison of Various Interpolated Temperature and Salinity Values at Standard Depths (Station 45, Bulgakov et al., 1965).

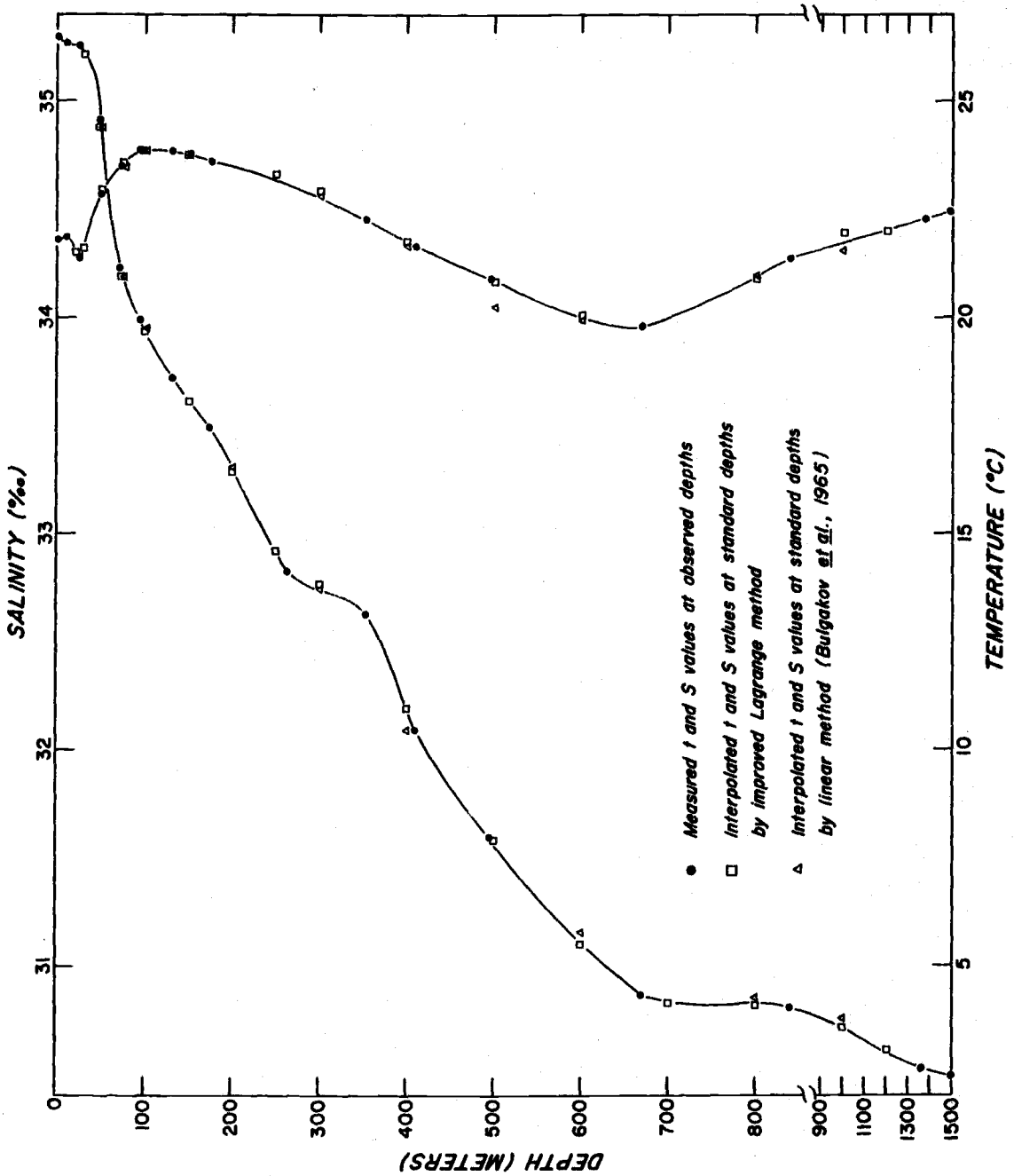
SALINITY (‰)
TEMPERATURE (°C)
DEPTH (METERS)
Measured t and S values at observed depths
Interpolated t and S values at standard depths by improved Lagrange method
Interpolated t and S values at standard depths by linear method (Bulgakov et al., 1965)

from the smooth profiles. This is the area where the sharp thermocline and halocline exist, and there are not data points near the depths in the vicinity of the sharp turning points. The missing data has a significant effect on the accuracy of Lagrange interpolations (Rattray, 1961).

Figures 5A and 5B show the sigma-t values at standard depths as calculated from the interpolated temperature and salinity values by two different interpolation methods. Also shown are those values of σ_t obtained by two interpolation methods from calculated sigma-t values at observed depths. It is clear that the differences of the two sigma-t values at standard depths as obtained by improved Lagrange interpolation are generally smaller than those by Bulgakov's piecewise linear interpolation. There are some exceptions at that layer of station 44 where significant deviations of interpolated temperature and salinity values appear. The computation of data by the improved Lagrange interpolation method at this station show that the effect on the difference of dynamic depth anomaly value accumulated in this layer alone amounts to 0.8 dyn cm.

However, from Table 6, one can see that if the improved Lagrange interpolation method is used, the difference between the currents based on density values obtained from temperature and salinity values interpolated to standard depths and currents based on interpolated density values calculated from the temperature and salinity values at

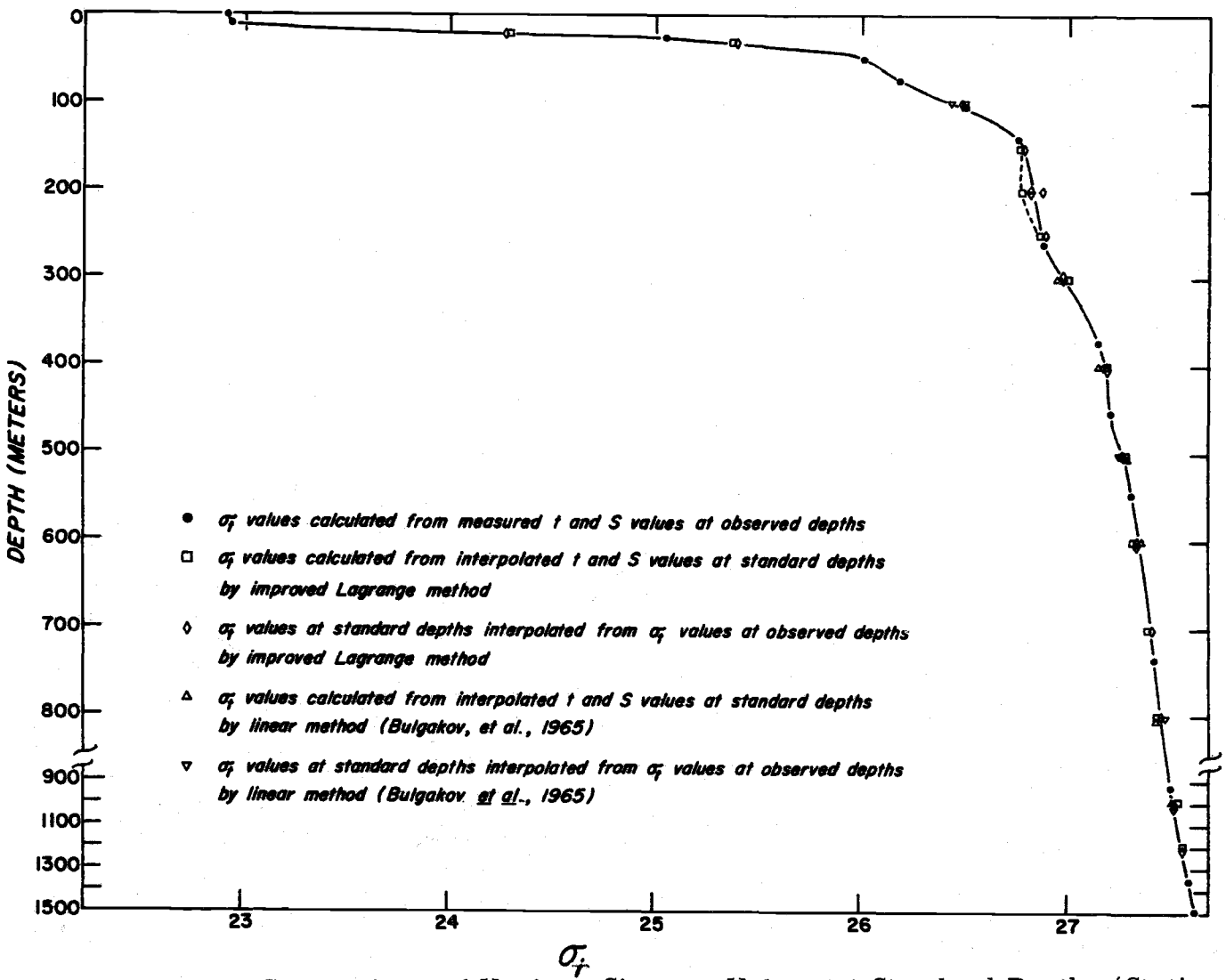

Figure 5A. Comparison of Various Sigma-t Values at Standard Depths (Station 44, Bulgakov et al., 1965).

Figure 5B. Comparison of Various Sigma-t Values at Standard Depths (Station 45, Bulgakov et al., 1965).

Table 6. Relative Difference in Magnitudes of Current Between Stations 44 and 45 (Bulgakov, et al. 1963) by Different Interpolation Procedures.

	A				B			
Z	V_1 cm/sec	V_2	ΔV	$\frac{\Delta V}{V_2}$ %	V_1	V_2	ΔV	$\frac{\Delta V}{V_2}$ %
0	105	102	3	3	100.9	100.2	0.7	0.7
10	104	101	3	3	100.3	99.6	0.7	0.7
25	102	98	4	4	99.0*	98.3	0.7	0.7
50	95	91	4	4	96.4	95.8	0.6	0.6
75	88	85	3	4	90.5	89.8	0.7	0.8
100	83	80	3	4	84.3	83.7	0.6	0.7
150	74	71	3	4	79.5	78.0	0.7	0.9
200	66	63	3	5	61.8	60.7	1.1	1.8
300	53	50	3	6	49.3	47.8	1.5	3.1
400	42	39	3	8	38.3	36.9	1.4	3.8
500	33	30	3	10	30.0	28.3	1.7	6
600	26	25	1	4	23.4	21.9	1.5	6.8
800	16	15	1	6	14.3	12.7	1.6	12.6
1000	10	9	1	10	8.6	7.2	1.4	19.4
1500	0	0	0	0	0	0	0	0

* = 30 meter depth.

V_1 = Current calculated from interpolated t, S value at standard depths.

V_2 = Current calculated from t, S values at observed depths.

Column A = Bulkagov's piecewise linear interpolation result.

Column B = Improved Lagrange interpolation result.

observed depths are not as significant as those presented by Bulgakov et al. (1963). The biggest difference here is only 1. 7 cm/sec with the improved Lagrange interpolation while the difference presented by them is as large as three to four cm/sec. This finding is consistent with that of the U. S. Naval office (1960).

This comparison leads to the belief that it is desirable to make a BT cast before each hydro-cast to detect the thermocline in the upper layer, and to place the Nansen bottles before and after the sharp turning point depths found in the BT trace. In this way, the interpolation problem in this area will be alleviated.

Discussion

From the preceding comparisons, one can see that the Hans Klein Chart has almost the same accuracy as the computer program in obtaining sea water density values. The use of H. O. tables yields results poorer than either of the above schemes due to the interpolations involved in each table. However, its problem of accuracy in this aspect is not significant enough to affect the dynamic depth anomaly calculation.

The error associated with the interpolation of hydro data is reflected in the difference between the density values calculated from temperature and salinity values interpolated to standard depths and the density values interpolated to standard depths after calculated

from temperature and salinity values at observed depths. If the improved Lagrange interpolation method is used and if proper sampling is conducted, this type of error is not significant in dynamic depth anomaly calculation when compared to the error caused by improperly choosing integration intervals. BT traces made before and during the hydro-cast can be used feasibly to aid in spacing the sample bottles so as to achieve good interpolation results and to supplement temperature structure detail in the upper layer. This procedure is important for obtaining accurate dynamic depth anomaly values.

Among the five data processing methods in this study, the fourth and fifth methods use graphic interpolation and include detailed temperature structure in the upper layer. They employ small integration intervals in the zone where the sharp thermocline appears. They may have some small plotting errors, but they would not yield the significant interpolation errors shown in the case of Figure 4A. Therefore, they appear to be the best choice for obtaining accuracy in dynamic depth anomaly computations. But, the fourth method uses thermosteric anomalies obtained from the Hans Klein Chart for dynamic depth anomaly calculations, and the effect of omitting pressure terms on current computations must be examined.

The first three methods use differently arranged computer programs. The first method does not yield as accurate sea water density values as does the second method. The third method is also better

than the second in this respect. However, they all suffer from a lack of judgement. By judgement is meant the use of synoptic interpretation for the handling of hydro-data which varies from time to time and station to station, and this judgement is needed in determining the integration intervals.

Based on this study of the overall effects on accuracy of computed geostrophic currents, the fifth method is considered the best one for data processing.

VI. ANALYSIS OF EFFECTS ON ACCURACY OF COMPUTED GEOSTROPHIC CURRENTS DUE TO THE PRACTICAL PROBLEMS IN DATA PROCESSING PROCEDURES

In analyzing the overall effects on accuracy of computed geostrophic currents due to the practical problems discussed in Chapter IV, four sets of data from a triangular set of 24 hour stations are used (Figure 2 and Table 1). Each of the four sets of data were selected so that the times of casts at each station were about the same time of day. These are called individual data sets. The currents computed from these four sets of data, processed by all the methods discussed in this study, are the surface currents relative to the 600 decibar level. This is the level of no motion, as defined by Defant (1961), for this area (Neshyba, 1967). The directions of current components are perpendicular to the three sides of the triangle of stations (Figure 2).

The currents so computed (Table 8) contain variations which are caused by internal waves of a predominantly 24-hour period. The fluctuations in dynamic depth anomaly by tide-excited internal waves are either diurnal or semidiurnal or both (Defant, 1950). Thus, the mathematical mean of the four sets of currents, for each leg of the triangle, should yield the mean geostrophic current components. It is understood that at least some of the variations can be a result of phenomena having periods greater than 24 hours; such variations

cannot be accounted for in this study.

Currents are computed by each of the methods described in Chapter V. Comparisons are made among the differences of the mean currents computed by these methods as well as the individual currents composing these means. The effects on accuracy of computed current are analyzed.

The Effect of Omitting Pressure Terms

The effect of omitting pressure terms in computed geostrophic currents is analyzed by comparing the differences between the currents computed by the fourth and fifth methods. The former uses thermosteric anomaly to calculate dynamic depth anomaly while the latter uses specific volume anomaly. The differences of the dynamic depth anomaly values at the 600 meter depth are given in Table 7. The mean values of the differences over 24 hours at three stations are 2.20, 2.09 and 2.16 dyn. cm., respectively. They can be considered constant.

Table 7. Difference of ΔD in Dyn Cm at the 600 Meter Depth Due to Omitting the Pressure Terms at Three 24-Hour Hydrography Stations.

Sta.	1st data set	2nd data set	3rd data set	4th data set	Mean
A	2.36	2.45	2.00	2.00	2.20
B	1.94	2.10	2.13	2.19	2.09
C	2.21	2.30	2.19	1.93	2.16

From Table 8, columns VI and V, one can see that the mean current components computed by these two methods are almost the same in all three legs. Currents computed from each of the individual data sets are also in general agreement, since the largest difference is only 0. 4 cm/sec (0. 3 dyn. cm of dynamic depth anomaly) and the average difference is only 0. 2 cm/sec. This is not significant compared to the measurement error of 1. 1 dyn. cm (Wooster et al., 1958) or even to the new standard of 0. 3 dyn. cm (Reed et al., 1966). This fact further points out that computed currents based on thermosteric anomalies alone can be accepted as accurate currents.

The Effect of Interpolating Hydro-Data

In Chapter V, it was shown that Lagrange interpolation is preferred over linear interpolation. This section discussed the error arising from Lagrange interpolation of t and S to observed depths vs. interpolation of δ to observed depths. This effect is studied by comparing the currents computed by the first and second methods (Table 8, column I and II). There is almost no difference in the mean currents obtained by these two methods. Among the individual sets of currents, the maximum difference is only 0. 5 cm/sec, and the average difference is 0. 2 cm/sec.

This comparison is consistent with the comparison made in the preceding chapter. However, for the purpose of obtaining accurate

Table 8. Surface Current Velocities (Cm/Sec) Relative to 600 Meter Depth Reference Level at 24 Hour Hydrographic Stations.

Legs	Data Set	Methods				
		I	II	III	IV	V
A-C	1	4.6	4.9	4.6	4.0	4.0
	2	4.1	4.3	3.8	3.6	3.8
	3	5.2	5.3	4.7	4.2	3.9
	4	5.1	5.3	4.4	5.7	5.8
	mean*	4.8	4.9	4.4	4.4	4.4
A-B	1	1.6	1.6	1.8	2.1	2.3
	2	2.9	2.6	2.7	1.9	2.3
	3	3.2	3.4	3.8	2.5	2.6
	4	4.4	4.2	4.3	5.8	5.6
	mean*	3.0	3.0	3.1	3.1	3.2
B-C	1	3.0	3.3	2.7	1.8	1.7
	2	1.2	1.7	1.1	1.6	1.5
	3	1.8	1.7	1.0	1.7	1.6
	4	0.7	1.1	0.1	-0.1	0.2
	mean*	1.7	1.9	1.3	1.3	1.2

* = Mathematical mean of four individual set currents.

A, B, C = Station designations.

sea water density values at standard depths, the improved Lagrange interpolation method still should be applied to the seawater density at observed depths instead of temperature and salinity at those depths.

The Effect of Missing Temperature Structure Detail in the Upper Layer

A comparison of the currents computed by the second and third methods shows the effect of missing temperature structure detail in the upper layer. Differences between the currents exist in the individual sets of currents as well as in the mean currents (Table 8, column II and III). The maximum difference among the individual sets of currents is 1.0 cm/sec and the average difference is 0.5 cm/sec. The differences between the mean currents are 0.5, 0.1, and 0.6 cm/sec. These differences are significant. It is clear that the added temperature detail from BT traces has its own virtue in improving the accuracy of geostrophic current computations.

The Effect of Selecting Integration Intervals

The differences between the currents computed by the third and fifth methods show the effects due to the selection of integration intervals. The third method uses the intervals between standard depths, and the fifth method uses small intervals in the area where the seawater density profile changes rapidly in relation to depth.

From Table 8, columns III and V, it is clear that there are a

number of differences among the sets of currents computed by these two methods. The maximum difference is 1.4 cm/sec and the average difference is 0.7 cm/sec. But, the mean currents are almost the same.

It appears that the selection of integration intervals has no significant effect on mean geostrophic current computations; but, for individual cases, it does have a strong effect on the accuracy of geostrophic current computations. In the study of the variations of current caused by internal waves, one cannot overlook such differences in the individual sets of currents. In most hydrographic surveys, only one set of data is normally obtained. This study shows the possibility that geostrophic currents so obtained may be significantly in error if this effect is not taken into account.

The Overall Effects

The overall effects on accuracy of computed geostrophic currents are best measured by the differences between the currents computed from the data processed by the first and fifth methods. The first method is used in most routine data processing, and it has the least ability in dealing with the practical problems studied in this paper. From the comparisons made in the preceding chapter, it is clear that the fifth method is the best choice for handling these practical problems. Its relatively poor results in seawater density calculations

have been found to be insignificant in obtaining dynamic depth anomalies. However, it has the disadvantage of being relatively time consuming.

In comparing the current computed by these two methods (Table 8, column I and V), it is seen that significant differences exist among the sets of currents. The average difference is 0. 7 cm/sec, and the maximum difference is 1. 3 cm/sec. For the mean currents, the differences are 0. 4, 0. 2 and 0. 5 cm/sec.

Deviations of the Individual Sets of Currents from the Mean Currents

A comparison of the magnitudes of deviations of individual sets of currents from the mean currents over 24 hours at each leg of the station triangle, is given in Table 9. It shows that the maximum ranges of the variations obtained by fifth method are 2. 0, 3. 3, and 2. 5 cm/sec for leg A-C, A-B, and B-C, respectively, while those obtained by the first method are 1. 0, 3. 0, and 2. 3 cm/sec. The second method yields variations similar to those of the first method, and the fourth method yields variations similar to those of the fifth method. The variations obtained by the third method stand by themselves with magnitudes of 0. 9, 2. 5, and 2. 6, respectively.

It is clear that the deviations of the individual set of current from the mean current show different magnitudes if the data is

Table 9. Deviations of Individual Currents (Cm/Sec) From the Mean Currents of the 24 Hour Hydrographic Stations.

Legs	Data Sets	Methods				
		I	II	III	IV	V
A-C	1	-0.2	0	0.2	-0.4	-0.4
	2	-0.7	-0.6	-0.6	-0.8	-0.6
	3	0.4	0.4	0.3	-0.2	-0.5
	4	0.3	0.4	0	1.3	1.4
A-B	1	-1.6	-1.4	-1.3	-1.0	-0.9
	2	-0.1	-0.4	-0.4	-1.2	-0.9
	3	0.2	0.4	0.7	-0.6	-0.6
	4	1.4	1.2	1.2	2.7	2.4
B-C	1	1.3	1.4	1.4	1.5	1.5
	2	0.5	0.2	0.2	0.2	0.3
	3	0.1	-0.2	-0.2	0.4	0.4
	4	-1.0	-0.8	-1.2	-1.4	-1.0

A, B, C = Station designations.

processed by different methods. Thus, for a study the variation caused by internal waves, data should be processed with the method which has the ability to yield correct results. The procedure presented by the fifth method is the best choice.

Discussion

From the comparison made in this chapter, it appears that unless the variations caused by internal waves can be averaged out with enough data, obtained over a sufficiently long period, the generally used data processing procedure presented in the first method does not have the ability to handle the problems caused by internal waves. The additional use of the temperature structure detail provided by BT traces alone does not yield high accuracy in geostrophic current computations unless small integration intervals are used to determine the mean sea water density in the area where the rapid change of density with depth appears as is done in the fifth method. Computer programs can be developed for the fifth method. But, it demands properly sampled data to avoid the error caused by the Lagrange interpolation used in computer programs.

VII. CONCLUSIONS

From the comparisons made in this study, the conclusions can be made that

1. Among the practical data processing schemes, the use of a computer program yields the best results for seawater density calculations, and the use of the Hans Klein Chart has better applicability in this aspect than the use of H. O. tables. However, the error from the use of H. O. tables is not significant enough to effect the dynamic depth anomaly calculations.
2. To obtain more accurate results in calculating seawater density values at standard depths, they should be calculated directly from measured values of temperature and salinity at observed depths and then reduced to standard depths instead of being calculated from interpolated temperature and salinity values.
3. The accuracy of dynamic depth anomaly computations depends on an understanding of the real oceanic structure. BT traces can help the Nansen bottle sampling scheme to some extent. BT casts should be made before and during each hydro-cast to provide information for bottle spacing and a more precise temperature profile.

4. With properly sampled data, the Lagrange interpolation method does not cause significant errors in dynamic depth anomaly calculations. There is no significant difference between the computed geostrophic currents based on density values obtained by interpolated temperature and salinity values and those based on interpolated density values.
5. In order to perform the dynamic depth anomaly numerical integration accurately, the selection of integration intervals should be based on the demands of each cast instead of using standard depth intervals for all cases. In other words, where changes of density are more rapid with respect to the depth, the interval should be smaller.
6. The Hans Klein Chart can yield enough information for on station planning of hydrographical work. It should be used to process data aboard ship as often as practically possible.

BIBLIOGRAPHY

Bjerknes, V. and J. W. Sandstrom. 1910. Dynamic meteorology and hydrography. Part I: Statistics. Washington, D. C. 146 p. (Carnegie Institution of Washington. Publication 88)

Bulgakov, N. P. and I F. Moroz. 1965. The reduction of specific volume of sea water to standard depths and its effect upon the accuracy of dynamic calculation. Academy of Science and the U. S. S. R., Oceanology 5(4):119-124. (Translated and produced by Scripta Technica Inc. for the American Geophysical Union)

California. University. Scripps Institution of Oceanography. 1966. Data report: Physical and chemical data, Boreas Expedition, 1966. (La Jolla) 164 pp. (SIO Reference 66-24)

Fomin, L. M. 1964. The dynamic method in oceanography. Amsterdam, Elsevier. 212 p.

Froese, C. 1960. Programs for oceanographic computations and data processing of the electronic digital computer ALWAC III-E. DP-3 Oceanographic station data program. Ottawa. 23 p. Canada. Fisheries Research Board. Manuscript report series (Oceanographic and Limnological) no. 73)

Defant, A. 1950. Reality and illusion in oceanographic surveys. Journal of Marine Research 9(2):120-138.

_____. 1961. Physical oceanography. Vol. 1. New York, Pergamon. 725 p.

Klein, Hans S. 1955. A new technique for processing physical oceanographic data. La Jolla, California, Scripps Institution of Oceanography. 15 p. (Manuscript)

Konaga, Shunji. 1965. The observation of the internal waves. The Oceanographical Magazine (Tokyo) 17(1-2):141-174.

LaFond, E. C. 1951. Processing oceanographic data. Washington, D. C., U. S. Naval Hydrographic Office. 113 p.

Leipper, Dale F. 1959. The classical hydrographical procedure and its relation to the physical and chemical properties of sea water. In: Proceeding of a Conference of Physical and Chemical Properties of Sea Water. Washington, D. C. p. 1-9. (National Research Council. Publication 600)

Montgomery, R. B. and E. D. Stroup. 1962. Equatorial waters and currents at 150° W. in July-August 1952. Baltimore, Johns Hopkins Press. 88 p. (Johns Hopkins Oceanography Studies no. 1)

Montgomery, R. B. and W. S. Wooster. 1954. Thermosteric anomaly and the analysis of serial oceanographic data. Deep Sea Research 2: 63-70.

Neshyba, Steve. 1967. Associate Professor, Oregon State University, Dept. of Oceanography. Personal communication. Corvallis, Oregon.

Neshyba, Steve and David E. Amstutz. 1965. Graphical aid for geostrophic computation from vertical sections. Deep Sea Research 12: 369-371.

Rattray, Maurice. 1962. Interpolation errors and oceanographic sampling. Deep Sea Research 9: 25-37.

Reed, R. K. and N. B. Laird. 1966. On the reliability of geostrophic flow determinations across a section of the North Pacific Ocean. Paper presented at the Pacific Northwest Regional Meeting of American Geophysical Union, Corvallis, Oregon, August. 7 p.

Sverdrup, H. U. 1947. Wind-driven currents in a baroclinic ocean, with application to the equatorial currents of the Eastern Pacific. Proceedings of National Academy of Sciences 33(11): 318-326.

U. S. Naval Hydrographic Office. 1960. A comparative study of three interpolation techniques used in processing oceanographic station data. Washington, D. C. 6 p. (Informal Oceanographic Manuscripts No. 28-60) (Unpublished manuscript)

Wooster, Warren S. and Bruce A. Taft. 1958. On the reliability of field measurements of temperature and salinity in the ocean. Journal of Marine Research 17: 552-556.

APPENDICES

APPENDIX I

FORTRAN, L, X, Computer Program of Oceanographic Data Processing (Sequence 447).

```
'SEQUENCE,447,  OCEANOGRAPHY
'FORTRAN,L,X
      PROGRAM HYDRO
      DIMENSION SD(26),MD(60),T(60),S(60),O(60),P(60),PH(60),A(60)
      DIMENSION F(60),D(60),AP(60),TT(60),SS(60),OO(60),PP(60),X(60)
      DIMENSION DEL(26),SIGMA(26),DYN(26),KD(26)
    4 FORMAT(R1,26X,I4,1X,2F5.3,8X,4F3.2)
  800 FORMAT(4X,A2,F3.1,A3,F3.1,3X,A2,2X,A2,A4,2X,2A3,2X,A3,2X,6A2,1X,
     12F3.1,4A2,I2,2A4)
  801 FORMAT(1H1,2A3,3X,A2,F5.1,2H N,3X,A3,F5.1,2H W,3X,5HDATE ,A2,1X,
     1A3,1X,A2,2X,A4,4H GCT,3X,5HWIRE ,A2,3X,3HDRY,F5.1,3X,3HWET,F5.1)
  802 FORMAT(1H ,15HWIND DIRECTION ,A2,5H VEL ,A2,4H KTS,4X,4HBAR ,A2,
     117H SWELL DIRECTION ,A2,3H H ,A2,3H T ,A2,7H CLOUD ,A2,5H AMT ,A2,
     2 9H WEATHER ,A2//)
  901 FORMAT(1H , I5,F8.2 ,F9.3,2F7.2,I9,F7.2,  F8.2,2F7.2,F8.2,F8.1,
     1F8.3)
  902 FORMAT(1H ,40X,I5,  F7.2,F8.2,2F7.2,F8.2,F8.1,F8.3)
  903 FORMAT(1H ,I5,F8.2,F9.3,2F7.2)
  702 FORMAT(  I5,F7.2,F8.2,2F7.2,F8.2,F8.1,F8.3,14X,2A4)
  904 FORMAT(I5,67X,2A4)
  905 FORMAT(1H1,10X,13HCARD COUNT IS,I10,//,9X,16HHEADING COUNT IS,I10)
      READ (1,904) NPCH
      SD(1) =0.
      SD(2)=10.
      SD(3)=20.
      SD(4)=30.
      SD(5)=50.
      SD(6)=75.
      SD(7)=100.
      SD(8)=150.
      SD(9)=200.
      SD(10)=250.
      SD(11)=300.
      SD(12)=400.
      SD(13)=500.
      SD(14)=600.
      SD(15)=700.
      SD(16)=800.
      SD(17)=1000.
      SD(18)=1200.
      SD(19)=1500.
      SD(20)=2000.
      SD(21)=2500.
      SD(22)=3000.
      SD(23)=4000.
      SD(24)=5000.
      SD(25)=6000.
      SD(26)=7000.
      AP(1)=.97264
      AP(2)=.972595
      AP(3)=.972550
      AP(4)=.972505
      AP(5)=.972415
      AP(6)=.9723025
      AP(7)=.97219
      AP(8)=.971965
      AP(9)=.97174
      AP(10)=.971515
      AP(11)=.97129
      AP(12)=.97084
```

```
      AP(13)=.9704
      AP(14)=.96995
      AP(15)=.96951
      AP(16)=.96907
      AP(17)=.96819
      AP(18)=.967320
      AP(19)=.96602
      AP(20)=.96388
      AP(21)=.96177
      AP(22)=.95970
      AP(23)=.95566
      AP(24)=.95173
      AP(25)=.94791
      AP(26)=.94421
      DO 900 I=1,26
  900 KD(I)=SD(I)
C  INITIALIZATION LOOP
    5 DO 85 I=1,60
      T(I)=0.
      S(I)=0.
      O(I)=0.
      P(I)=0.
      PH(I)=0.
      PP(I)=0.
      OO(I)=0.
      X(I)=0.
      MD(I)=0.
   85 A(I)=0.
      ICNT=1
      Q=0.
C  INPUT - NSTOP=NUMBER OF DEPTHS FOR WHICH THERE ARE OBSERVATIONS
      READ(1,800)L,XL,G,XM,IY,ND,NT,S1,S2,XD,IZ,IH,IP,IW,IF,IB,TD,TW,
     1IL,IN,IA,NA,NSTOP,ICR,IST
      IF(NSTOP.EQ.0)999,851
  851 N=0
  852 READ(1,4)ICK,MD(N+1),T(N+1),S(N+1),O(N+1),P(N+1),PH(N+1),A(N+1)
      IF(ICK.EQ.1R )854,853
  853 N=N+1
      GO TO 852
  854 IF(N.NE.NSTOP)855,856
  855 PRINT 905,N,NSTOP
      GO TO 5
  856 NSTOP=N
      N=0
    9 ID=1
      R=0.
C   CONSTRUCTION OF VECTORS.  MISSING VALUES ELIMINATED IN DO-LOOP  STARTING
C   IN STATEMENT 10
      GO TO (14,11,12,13),ICNT
   14 DO 24 I=1,NSTOP
   24 X(I)=T(I)
      GO TO 10
   11 DO 21 I=1,NSTOP
   21 X(I)=S(I)
      GO TO 10
   12 DO 22 I=1,NSTOP
   22 X(I)=O(I)
      GO TO 10
   13 DO 23 I=1,NSTOP
   23 X(I)=P(I)
```

```
   10 K=0
      DO 29 I=1,NSTOP
      IF(X(I)) 28,29,28
   28 K=K+1
      F(K)=X(I)
      D(K)=MD(I)
   29 CONTINUE
C  SCHEME TO FIND POINTS TO USE  IN THE INTERPOLATION
      KK=K-1
      IF(K-3) 36,36,30
   30 IF(D(1)-R)31,49,34
   31 IF(D(2) - R) 32,50,37
   32 DO 33 I=3,KK
      IF(D(I)-R) 33,52,39
   33 CONTINUE
      IF(D(K)-R+Q) 69,51,38
   37 M=1
      F1=F(1)
      F2=F(2)
      F3=F(3)
      D1=D(1)
      D2=D(2)
      D3=D(3)
      GO TO 40
   38 M=1
      F1=F(KK-1)
      F2=F(KK)
      F3=F(KK+1)
      D1=D(KK-1)
      D2=D(KK)
      D3=D(KK+1)
      GO TO 40
   39 M=0
      F1=F(I-2)
      F2=F(I-1)
      F3=F(I)
      F4=F(I+1)
      D1=D(I-2)
      D2=D(I-1)
      D3=D(I)
      D4=D(I+1)
C  INTERPOLATION BLOCK.  PTRP=P123, PT=P234, XMAX= THE VALUE OF D FOR WHICH PTRP
C  OR PT IS A MAXIMUM.  IF THIS VALUE FALLS INSIDE THE INTERPOLATION INTERVAL
C  LINEAR INTERPOLATION IS USED PROVIDED THE INTERPOLATION IS NOT BETWEEN
C  THE TWO ADJACENT OBSERVED VALUES.
   40 PTRP=F1*(D2-R)*(D3-R)/((D2-D1)*(D3-D1))
      PTRP = PTRP + F2*(D1-R)*(D3-R)/((D1-D2)*(D3-D2))
      PTRP=PTRP + F3*(D1-R)*(D2-R)/((D1-D3)*(D2-D3))
      XMAX=.5*((D1**2)*(F3-F2)+(D2**2)*(F1-F3)+(D3**2)*(F2-F1))
      XMAX=XMAX/(D1*(F3-F2)+D2*(F1-F3)+D3*(F2-F1))
      IF(D2-XMAX)101,101,103
  101 IF(D3-XMAX) 103,102,102
  102 JJ=1
  103 IF(M) 42,41,42
   41 PT=F2*(D3-R)*(D4-R)/((D3-D2)*(D4-D2))
      PT=PT + F3*(D2-R)*(D4-R)/((D2-D3)*(D4-D3))
      PT=PT + F4*(D2-R)*(D3-R)/((D2-D4)*(D3-D4))
      XMAX=.5*((D2**2)*(F4-F3)+(D3**2)*(F2-F4)+(D4**2)*(F3-F2))
      XMAX=XMAX/(D2*(F4-F3)+D3*(F2-F4)+D4*(F3-F2))
      IF(D2-XMAX) 104,104,99
```

```
  104 IF(D3-XMAX) 99,105,105
  105 JJ=1
   99 PTRP=(PT+PTRP)/2.
   42 IF(JJ-1) 109,110,109
  110 IF(PTRP-F2) 106,109,108
  106 IF(PTRP-F3) 107,109,109
  108 IF(PTRP-F3) 109,109,107
  107 PTRP=(F3-F2)*(R-D2)/(D3-D2) +F2
  109 GO TO (43,44,45,46),ICNT
   43 TT(ID)=PTRP
      GO TO 34
   44 SS(ID)=PTRP
      GO TO 34
   45 OO(ID)=PTRP
      GO TO 34
   46 PP(ID)=PTRP
      GO TO 34
   49 I=1
      GO TO 52
   50 I=2
      GO TO 52
   51 I=K
   52 GO TO (53,54,55,56), ICNT
   53 TT(ID)=F(I)+.005
      GO TO 34
   54 SS(ID)=F(I)+.005
      GO TO 34
   55 OO(ID)=F(I)+.005
      GO TO 34
   56 PP(ID)=F(I)+.005
      GO TO 34
C  BLOCK OF TRANSFERS.  ID IS A COUNTER ON THE NUMBER OF STANDARD DEPTHS FOR
C  WHICH INTERPOLATIONS ARE MADE FOR A GIVEN PROPERTY.  N IS THE MAXIMUM ID FOR
C  THE STATION.  ICNT KEEPS TRACK OF WHICH PROPERTY IS BEING PROCESSED.
C  Q IS A DUMMY VARIABLE USED TO ALLOW EXTRAPOLATION WHEN IT IS FEASIBLE.
   69 ID=ID-1
   60 IF(ID-N) 36,36,61
   61 N=ID
   36 IF(ICNT-4) 71,70,70
   71 ICNT=ICNT+1
      GO TO 9
   35 ID = ID +1
      R=SD(ID)
      Q=0.0
      IF(ID.LT.8)30,80
   80 IF(ID.LT.11)81,82
   81 Q=5.1
      GO TO 30
   82 IF(ID.LT.13)83,84
   83 Q=10.1
      GO TO 30
   84 IF(ID.LT.14)185,86
  185 Q=15.1
      GO TO 30
   86 IF(ID.LT.16)87,88
   87 Q=20.2
      GO TO 30
   88 IF(ID.LT.17)89,90
   89 Q=25.1
      GO TO 30
```

```
   90 Q=30.1
      GO TO 30
   34 IF(ID-26) 35,60,60
C    COMPUTATION BLOCK.  SIGMA-T,DELTA, AND DYNAMIC HEIGHT ARE COMPUTED AT
C    STANDARD DEPTHS
   70 DH=0.
      PREV=0.
      PREVD=0.
      DO 123 I=1,N
      Z=SD(I)
      R=TT(I)
      W=SS(I)
      CL=(W-.03)/(1.805)
      SSOO=((.0000398*CL-.00157)*CL + 1.4708)*CL -.069
      BT=1.E-6*R*((.01667*R-.8164)*R+18.03)
      AT=.001*R*((.0010843*R-.09818)*R+4.7867)
      SUMT=(R-3.98)*(R-3.98)*(R+283.)/(503.57*(R+67.26))
      SSTO=(SSOO+.1324)*(1.-AT+BT*(SSOO-.1324))-SUMT
      ASTO=1./(SSTO*.001 +1.)
      V=4886./(1.+.0000183*Z)
      B=((.004*R-.551)*R+28.33)*R+227.
      C=(.158*R+9.5)*R + 105.5
      XX=(.04*R-2.72)*R +147.3-Z*1.E-4*((.002*R-.87)*R +32.4)
      E=4.5+.1*R-Z*1.E-4*(1.8-.06*R)
      Q=(SSOO-28.)*.1
      Q=(-1.5E-8*R*Z+C*1.E-4)*Z+(E*Q-XX)*Q
      ASTP=ASTO*(1.-Z*1.E-9*(Q+V-B))
      DELTA=ASTP - AP(I)
      DD=.5*(DELTA+PREVD)*(Z-PREV)
      DH=DH+DD
      DYN(I)=DH
      PREV=Z
      PREVD=DELTA
      DEL(I)=DELTA*1.E+5+.05
  123 SIGMA(I)=SSTO+0.005
C   OUTPUT BLOCK
      IF(NPCH.EQ.0)950,1234
 1234 WRITE(2,904)N,ICR,IST
  950 WRITE(3,801) S1,S2,L,XL,G,XM,ND,XD,IY,NT,NA,TD,TW
      WRITE(3,802)IW,IF,IB,IZ,IH,IP,IN,IA,IL
      IF(NSTOP-N) 202,203,204
  202 K=1
      LN=NSTOP
      LM=N
      GO TO 205
  203 K=2
      LN=NSTOP
      GO TO 205
  204 K=3
      LN=N
      LM=NSTOP
  205 WRITE(3,901)(MD(I),T(I),S(I),O(I),P(I),KD(I),TT(I),SS(I),OO(I),
     1PP(I),SIGMA(I),DEL(I),DYN(I),I=1,LN)
      IF(NPCH.EQ.0)960,2051
 2051 WRITE(2,702)                                (KD(I),TT(I),SS(I),OO(I),
     1PP(I),SIGMA(I),DEL(I),DYN(I),ICR,IST,I=1,LN)
  960 GO TO(206,5,208),K
  206 LN=LN+1
      WRITE(3,902)(KD(I),TT(I),SS(I),OO(I),PP(I),SIGMA(I),DEL(I),DYN(I),
     1I=LN,LM)
```

```
      IF(NPCH.EQ.0)5,2061
 2061 WRITE(2,702)(KD(I),TT(I),SS(I),OO(I),PP(I),SIGMA(I),DEL(I),DYN(I),
     1ICR,IST,I=LN,LM)
      GO TO 5
  208 LN=LM+1
      WRITE(3,903)(MD(I),T(I),S(I),O(I),P(I),I=LN,LM)
      GO TO 5
  999 END
```

APPENDIX II

FORTRAN, L, X, Computer Program of Oceanographic Data Processing (Sequence 852).

```
'SEQUENCE,852,  OCEANOGRAPHY
'FORTRAN,L,X

      PROGRAM HYDRO1
C        COMPUTES SIGT AND DELTA FROM OBSERVED DATA AND THEN INTERPOLATES
C
      DIMENSION OD(50),OSIG(50),OT(50),OSAL(50),ODEL(50),ODELD(50),SD(30
     1),SSIG(30),ST(30),          SSAL(30),SDEL(30),SDELD(30)
      DIMENSION PODEL(50),PSDEL(30)
      READ 101, SD
  101 FORMAT (5F16.0)
    1 READ 102, L,XL,G,XM,IY,ND,NT,S1,S2,XD,IZ,IH,IP,IW,IF,IB,TD,TW,IL,I
     1N,IA,NA,NSTOP,ICR,IST
  102 FORMAT(4X,A2F3.1,A3,F3.1,3X,A2,2X,A2,A4,2X,2A3,2X,A3,2X,6A2,1X,
     12F3.1,4A2,I2,2A4)
      IF(NSTOP.EQ.0) 17,2
    2 N=0
    3 READ 103,ICK,OD(N+1),OT(N+1),OSAL(N+1)
  103 FORMAT(R1,26X,F4.0,1X,2F5.3)
      IF(ICK.EQ.1R ) 5,4
    4 N=N+1
      GO TO 3
    5 IF(N.NE.NSTOP) 6,7
    6 PRINT 104, N, NSTOP
  104 FORMAT(/////,10X,10HCARD COUNT,I5,//, 10X,12HHEADER COUNT,I5,////)
    7 DO 8 K=1,N
      T=OT(K)
      S=OSAL(K)
      Z=OD(K)
      CL=(S-0.03)/1.805
      SIG0=((0.0000398*CL-0.00157)*CL+1.4708)*CL-0.069
      CSIGT=(T-3.98)**2*(T+283.0)/(T+67.26)/503.57
      BT=T*1.0E-6*(18.03-T*(0.8164-0.01667*T))
      AT=T*1.0E-3*(4.7867-T*(0.09818-0.0010843*T))
      SIG=OSIG(K)=(SIG0+0.1324)*(1.0-AT+BT*(SIG0-0.1324))-CSIGT
      ALPHST0=1.0/(1.0+1.0E-3*SIG)
      V=4886.0/(1.0+0.0000183*Z)
      B=((0.004*T-0.551)*T+28.33)*T+227.0
      C=(0.158*T+9.5)*T+105.5
      XX=(0.040*T-2.72)*T+147.3-1.0E-4*Z*((0.002*T-0.87)*T+32.4)
      E=4.5+0.1*T-1.0E-4*Z*(1.8-0.06*T)
      Q=0.1*(SIG0-28.0)
      Q=(-1.5E-8*T*Z+1.0E-4*C)*Z+(E*Q-XX)*Q
      ALPHSTP=ALPHST0*(1.0-1.0E-9*Z*(Q+V-B))
      ALPH350P=0.972643-0.972643*Z*(4886.0/(1.0+0.0000183*Z)-227.0+
     1  0.01055*Z-0.126*(14.730-0.000324*Z))*1.0E-9
      ODEL(K)=ALPHSTP-ALPH350P
    8 PODEL(K)=ODEL(K)*1.0E5
      C=ODELD(1)=0.0
      DO 9 K=2,N
    9 C=ODELD(K)=C+(OD(K)-OD(K-1))*(ODEL(K)+ODEL(K-1))/2.0
      K=0
   10 K=K+1
      IF(SD(K).GT.OD(N)) 11,12
   11 IF(ABS(SD(K)-OD(N)).LT.0.1*(OD(N)-OD(N-1))) 12,13
   12 ST(K)=VAL(  N,SD(K),OD,OT)
      SSAL(K)=VAL(N,SD(K),OD,OSAL)
      SSIG(K)=VAL(N,SD(K),OD,OSIG)
      SDEL(K)=VAL(N,SD(K),OD,ODEL)
      PSDEL(K)=SDEL(K)*1.0E5
```

```
      GO TO 10
   13 M=K-1
      C=SDELD(1)=0.0
      DO 14 K=2,M
   14 C=SDELD(K)=C+(SD(K)-SD(K-1))*(SDEL(K)+SDEL(K-1))/2.0
      PRINT 105,S1,S2,L,XL,G,XM,ND,XD,IY,NT,NA,TD,TW,IW,IF,IB,IZ,IH,IP,
     1 IN,IA,IL
  105 FORMAT(1H1,2A3,3X,A2,F5.1,2H N,3X,A3F5.1,2H W,3X,5HDATE ,A2,1X,A3,
     11X,A2,2X,A4,4H GCT,3X,5HWIRE ,A2,3X,3HDRY,F5.1,3X,3HWET,F5.1,/,1X,
     215HWIND DIRECTION ,A2,5H VEL ,A2,4H KTS,4X,4HBAR ,A2,17H SWELL DIR
     3ECTION ,A2,3H H ,A2,3H T ,A2,7H CLOUD ,A2,5H AMT ,A2,9H WEATHER ,
     4 A2,//)
      L=MIN0(M,N)
      PRINT 106,(OD(K),OT(K),OSAL(K),OSIG(K),PODEL(K),ODELD(K),SD(K),ST(
     1K),SSAL(K),SSIG(K),PSDEL(K),SDELD(K),K=1,L)
  106 FORMAT(2(10X,F4.0,F8.2,F9.3,F8.2,F9.1,F8.3))
      IF(N.EQ.L) 16,15
   15 L=L+1
      PRINT 107,(OD(K),OT(K),OSAL(K),OSIG(K),PODEL(K),ODELD(K),K=L,N)
  107 FORMAT(10X,F4.0,F8.2,F9.3,F8.2,F9.1,F8.3)
      GO TO 1
   16 L=L+1
      PRINT 108,(SD(K),ST(K),SSAL(K),SSIG(K),PSDEL(K),SDELD(K),K=L,M)
  108 FORMAT(66X,F4.0,F8.2,F9.3,F8.2,F9.1,F8.3)
      GO TO 1
   17 END

      FUNCTION VAL(N,XO,X,F)
      DIMENSION X(1),F(1)
      DO 1 I=1,N
      IF(XO.GE.X(I)) 1,2
    1 CONTINUE
      I=N
    2 IF(I.EQ.N) 3,4
    3 VAL=F(I-2)*(X(I-1)-XO)*(X(I)-XO)/(X(I-1)-X(I-2))/(X(I)-X(I-2))
     1+F(I-1)*(X(I-2)-XO)*(X(I)-XO)/(X(I-2)-X(I-1))/(X(I)-X(I-1))
     1+F(I)*(X(I-2)-XO)*(X(I-1)-XO)/(X(I-2)-X(I))/(X(I-1)-X(I))
      RETURN
    4 IF(I.LT.3) 5,6
    5 I=3
      GO TO 3
    6 VAL=0.5*(F(I-2)*(X(I-1)-XO)*(X(I)-XO)/(X(I-1)-X(I-2))/(X(I)-X(I-2)
     1)+F(I-1)*(X(I-2)-XO)*(X(I)-XO)/(X(I-2)-X(I-1))/(X(I)-X(I-1))
     1+F(I)*(X(I-2)-XO)*(X(I-1)-XO)/(X(I-2)-X(I))/(X(I-1)-X(I))
     1+F(I-1)*(X(I)-XO)*(X(I+1)-XO)/(X(I)-X(I-1))/(X(I+1)-X(I-1))
     1+F(I)*(X(I-1)-XO)*(X(I+1)-XO)/(X(I-1)-X(I))/(X(I+1)-X(I))
     1+F(I+1)*(X(I-1)-XO)*(X(I)-XO)/(X(I-1)-X(I+1))/(X(I)-X(I+1)))
      END
```

APPENDIX III
Hans Klein Chart